Open Access
Earth System
Science
Data
Discussions

1 **MUDA: dynamic geophysical and geochemical MUltiparametric DAtabase**

Marco Massa [1], Andrea Luca Rizzo [1,2], Davide Scafidi [3], Elisa Ferrari [1], Sara Lovati [1], Lucia Luzi [1] and MUDA WG (*)

2

3 [1] National Institute of Geophysics and Volcanology (INGV), Milano department, Italy

[2] University of Milano Bicocca, DISAT, Milano, Italy

[3] University of Genova, DISTAV, Genova, Italy

4

5 (*) A full list of authors appears at the end of the paper

6

7 Corresponding author: marco.massa@ingv.it

8

9 **Abstract**

10   In this paper, the new dynamic geophysical and geochemical MUltiparametric DAtabase

11 (MUDA) is presented. MUDA is a new infrastructure of the National Institute of Geophysics and

12 Volcanology (INGV), published on-line in December 2023, with the aim of archiving and

13 disseminating multiparametric data collected by multidisciplinary monitoring networks. MUDA is a

14 *MySQL* relational database with a web interface developed in *php,* aimed at investigating in quasi real

15 time possible correlations between seismic phenomena and variations in endogenous and

16 environmental parameters. At present, MUDA collects data from different types of sensors such as

17 hydrogeochemical probes for physical-chemical parameters in waters, meteorological stations,

18 detectors of air Radon concentration, diffusive flux of carbon dioxide (CO_2) and seismometers

19 belonging both to the National Seismic Network of INGV and to temporary networks installed in the

20 framework of multidisciplinary research projects. MUDA daily publishes data updated to the previous

21 day and offers the chance to view and download multiparametric time series selected for different

22 time periods. The resultant dataset provides broad perspectives in the framework of future high

23 frequency and continuous multiparametric monitorings as a starting point to identify possible seismic

24 precursors for short-term earthquake forecasting. MUDA is now quoted with the Digital Object

25 Identifier https://doi.org/10.13127/muda (Massa et al., 2023).

26

27 **Key words:** multiparametric data, monitoring networks, dynamic data base, earthquakes forecasting

28

29 **1 Introduction**

30

31 Today, the increasing awareness on the interaction between tectonics and crustal fluids

32 dynamics is still lacking a simultaneous monitoring of the relative key factors. Changes in water

33 chemistry and levels, spring discharges, soil flux regimes (e.g. CO_2, CH_4, Radon) and compositions

34 of dissolved gases in water are well-documented in the literature (e.g. Italiano et al., 2001, 2004;

35 Chiodini et al., 2020; Gori and Barberio, 2022 and references therein), as being pre-, co- and post-

36 seismic modifications as well as markers of the local tectonic stress acting in the crust. These

37 recognized seismic-induced variations in groundwaters and springs led, in recent years, scientists to

38 give more attention to the development of multiparametric monitoring, in order to capture the main

39 evidence concerning abrupt changes in chemical and physical parameters recorded before (and also

40 after) energetic seismic events (Rikitake and Hamada, 2003; Cicerone et al., 2009; Martinelli, 2018

41 and references therein). The ultimate goal is to find systematic signals that can be assumed as possible

42 "precursors" or indicators that a seismogenetic process is ongoing (Hubbert and Rubey, 1959; Brauer

43 et al., 2003; Miller et al., 2004; Chiarabba et al., 2009; Di Luccio et al., 2010; Malagnini et al., 2012;

44 Keranen and Weingarten, 2018; Napolitano et al., 2020; De Matteis et al., 2021; Gabrielli et al., 2022,

45 2023; Ventura and Di Giovambattista, 2013). At the Italian scale, several studies have described the

46 utility of groundwater and spring parameters and soil gas emissions to catch seismic-related signals

47 as well. However, only a few studies reported a continuous, high-frequency monitoring, mainly of

48 groundwater level or hydraulic pressure (De Gregorio et al., 2012; Barberio et al., 2017; De Luca et

49 al., 2018), or as Gori and Barberio (2022) concerning spring monitoring (i.e. temperature, pH,

50   electrical conductivity, dissolved oxygen and carbon dioxide) or D'Alessandro et al. (2020) on soil

51   radon emissions related to seismic activity.

52   MUDA (geophysical and geochemical MUltiparametric DAtabase), a new dynamic

53   multiparametric database published on-line in December 2023 at the web site https://muda.mi.ingv.it

54   (Figure 1), has been developed in such a framework. MUDA is a new infrastructure of the National

55   Institute of Geophysics and Volcanology (INGV, www.ingv.it) devoted to archive daily and distribute

56   quasi real time geophysical and geochemical multiparametric data recorded in continuous or near-

57   continuous mode at selected sites installed at the most tectonically active Italian areas (Figure 2).

58   MUDA was designed in the framework of INGV Dynamic Planet S2-project (i.e. 3D structure of Italy

59   from multidata analysis. Passive/active seismic, magnetic, magnetotelluric, electrical, gravimetric

60   prospecting, https://progetti.ingv.it/it/pian-din) and its development is ongoing in the framework of

61   the INGV Dynamic Planet GEMME project (Integrated Geological, gEophysical and geocheMical

62   approaches for 3D Modelling of complex seismic site Effects).

63   The need for an infrastructure capable of acquiring, storing, organising and publishing

64   multiparameter data in near real time arose following the installation of the Garda multiparameter

65   seismic network, PDnet (https://eida.ingv.it/it/networks/network/ZO), installed starting from 2021 as

66   part of the Task-S2 of the INGV Dynamic Planet project (Massa et al., 2021; Ferrari et al., 2024). In

67   this framework, MUDA collects information from different types of sensors, such as seismometers,

68   accelerometers, hydrogeochemical for physical-chemical parameters in waters, geochemical for

69   measuring the diffusive flux of carbon dioxide (CO_2) from the soil or detecting the air Radon

70   concentration, and meteorological stations. The aim is to constraint the influence due to exogenous

71   parameters in order to make potential correlations between seismic phenomena and variations

72   concerning monitored parameters (i.e. groundwater level, temperature, electrical conductivity, CO_2

73   soil flux, air Radon concentration; Barberio et al., 2017; Chiodini et al., 2020; Mastrorillo et al.,

74   2020).

75   The challenge of MUDA is to provide the end-user a high quality dynamic but also

76   simultaneous and continuous monitoring of groundwater physical parameters, meteorological data

77   and seismic signals, together with gas concentration such as Radon or soil CO_2-CH_4 fluxes (Figure

78   3). In order to furnish the main information for a detailed interpretation of local phenomena in the

79   framework of multihazard assessment, the multiparametric data are provided together with all

80   necessary stations and sites metadata, supplied with a complete geological and morphological

81   description (Figure 4).

82

83   2 Seismotectonic framework and seismicity

84

85   The multiparametric sites now included in MUDA are located in five main target areas (Figure

86   2): Lake Garda, eastern Alps, Po alluvial basin and Northern and Central Apennine chains (Table 1).

87   Concerning instrumental seismicity (http://terremoti.ingv.it/), in the last 40 years, thousands of small

88   to moderate energy seismic events (Figure 2) occurred in Northern Italy. Despite the low-to-medium

89   seismic hazard of the area (Stucchi et al., 2011), the high level of exposure (e.g. metropolitan areas,

90   industrial plants etc.), the local geological condition and the proximity of active buried seismogenic

91   structure (Burrato et al., 2012) make many portions of North Italy a medium to high seismic risk zone

92   (Massa et al., 2022b, Lai et al., 2020).

93   In particular, the Garda region (Area 1, Figure 2) is characterized by low-to-moderate

94   seismicity with the active tectonic regime located on the margin of the southern Alpine chain

95   controlled by the Africa-Europe convergence. The main active faults affecting the area consist of

96   mainly NNE-SSW trending thrusts (Galadini et al., 2001). For instance, the November 24, 2004,

97   Vobarno M_w 4.8 earthquake (https://terremoti.ingv.it/event/1564989), generated maximum

98   macroseismic intensities (Imax) of VII/VIII (https://emidius.mi.ingv.it/CPTI15-DBMI15/, Locati et

99   al., 2022). It is worth noting that in the past the same area was struck by several powerful events, such

100 as the October 30th, 1901 Salò M_w=5.4 earthquake (https://emidius.mi.ingv.it/CPTI15-DBMI15/,

101 Rovida et al., 2022).

102 Moving eastwards (Area 2, Figure 2), the highest rate of energetic events in Northern Italy is

103 associated to the South-verging thrust faults typical of the central and East South Alpine Chain

104 (Battaglia et al., 2004; Serpelloni et al., 2005; D'Agostino et al., 2008), due to the North-South

105 convergence between the Adriatic microplate and the Alps. The most recent destructive earthquake

106 occurred in Friuli, during the seismic sequence of May 6, 1976, with M_w= 6.5 (Pondrelli et al., 1999

107 and reference therein), whereas the largest historical event was the 1695 Asolo earthquake, with an

108 estimated M_w=6.48 (https://emidius.mi.ingv.it/CPTI15-DBMI15/) broadly associated to the thrust

109 system of the Montello area (Danesi et al., 2015).

110 South of the Alps, the Po alluvial plain (Area 3, Figure 2) represents a very deep foreland

111 basin of two opposing verging fold-and-thrust belts developing in the framework of the African and

112 European plates relative convergence (Pieri and Groppi, 1981; Bigi et al., 1990). Despite the flat

113 morphology, the Po plain is far from being an undeformed domain, since the outermost and most

114 recent thrust fronts of the two belts are buried by the Plio-Quaternary sedimentary sequence (Burrato

115 et al., 2012). The historical and instrumental Italian seismic catalogues show that the southern Po

116 plain is affected by low to moderate seismicity, with M_w up to 5.8 during the 2012 sequence (Luzi et

117 al., 2013). Considering the historical seismicity (Rovida et al., 2020), the central part of the Po plain

118 was struck by the more significant North Italy earthquake on January 3, 1117, with an estimated

119 M_w=6.52.

120 Moving southwards, the Northern Apennines (Area 4, Figure 2) underwent the regional

121 seismicity associated with the Apennine fronts defined by different arcs of blind, North-verging

122 thrusts and folds (Mazzoli et al., 2015; Chiaraluce et al., 2017), capable of generating moderate

123 energetic seismic events with a maximum magnitude around 6 (i.e. June 5, 1501, M_w 6.05, Rovida et

124 al., 2022). In particular, this area hosts the Nirano site (Table 1), in the Regional Natural Reserve of

125 Salse di Nirano (Giambastiani et al., 2024; Romano et al., 2023), an area lying upon an anticline

126   structure of the North-East verging fold-and-thrust Apennine belt characterized by one of the largest

127   mud volcano fields in Europe (Bonini, 2008; Castaldini et al., 2005) coupled to the emission of CH_4-

128   dominated gases (e.g., Buttitta et al., 2020).

129   Finally, two stations included in MUDA, are installed in the surroundings of the Norcia

130   alluvial basin (Area 5, Figure 2), an area characterized by high seismic hazard and seismicity rate due

131   to dense extensional NW-SE active fault systems (e.g. Galadini et al., 1999, Brozzetti and Lavecchia,

132   1994) capable of generating high-magnitude earthquakes (Galli et al., 2018; 2019), such as the

133   January 14, 1703, M_w=6.9, earthquake or other moderate events such as the 1328, M_w=6.3, the 1730,

134   M_w=5.9, the 1859, M_w=5.5 and the 1979, M_w=5.8, earthquakes (Rovida et al, 2022). The recent

135   instrumental seismicity highlights the two main events occurring on August 24, 2016 and on the

136   October 30, 2016, with M_w 6.0 and 6.5 respectively, in an area a few kilometres of the Norcia plain

137   (e.g. Improta et al., 2019 and reference therein).

138

139   **3 State of the art**

140

141   At present, in Italy and Europe, the seismological communities in general are fairly advanced

142   in their running of both network data management and seismic data sharing. In Italy, the main seismic

143   network   is   represented   by   the   National   Seismic   Network   (RSN,

144   https://eida.ingv.it/it/networks/network/IV, Margheriti et al., 2020), managed by INGV and

145   sometimes integrated for real time data exchange by many local or regional networks (Massa et al.,

146   2022). The RSN permanent network is codified through the IV code assigned by the International

147   Federation of Digital Seismograph Networks, FDSN (https://www.fdsn.org/). The RSN station codes

148   are registered at International Seismological Center, ISC (http://www.isc.ac.uk/), while data, recorded

149   following   the   SEED   (Standard   for   the   Exchange   of   Earthquake   Data,

150   http://www.fdsn.org/seed_manual/SEEDManual_V2.4.pdf) format, are shared (Danacek et al., 2022)

151   through the EIDA-Italia node (European Integrated Data Archive, https://eida.ingv.it/it/). In Italy,

152   INGV provides many websites and thematic databases for real time data quality and distribution,

153   such as EIDA-Italia, ISMDq (INGV Strong Motion Data quality, https://ismd.mi.ingv.it , Massa et

154   al., 2022), ITACA (ITalian Accelerometric Archive, https://itaca.mi.ingv.it, Pacor et al., 2011), ESM

155   (Engineering Strong Motion database, https://esm-db.eu/, Luzi et al., 2016), BSI (Italian Seismic

156   Bulletin, https://terremoti.ingv.it/bsi, Marchetti et al., 2016), TDMT (Time Domain Moment Tensor,

157   https://terremoti.ingv.it/tdmt, Scognamiglio et al., 2009), ShakeMaps (https://shakemap.ingv.it/,

158   Michelini et al., 2020), etc.

159   Differently, the geochemical community has still not developed a so capillary network of automatic

160   stations for data acquisition, management and sharing, as the seismic community does. This mostly

161   depends on the fact that only a few geochemical parameters/tracers can be measured directly in the

162   field and in near real-time [e.g., diffusive flux of CO_2 from the soil through accumulation chamber

163   method (Chiodini et al., 1998; Carapezza et al., 2004; Inguaggiato et al., 2011a; Rizzo et al., 2015),

164   radon concentration in atmosphere or from the soil with specific Geiger counters, concentration of

165   H_2O, CO_2, SO_2, H_2S, CH_4, halogens in atmosphere through MULTIGAS sensors (Aiuppa et al., 2005;

166   Shinohara et al., 2005) or FTIR technique (e.g., Allard et al., 2005), SO_2 flux in atmosphere by DOAS

167   and UV techniques (Burton et al., 2009; Aiuppa et al., 2021)]. It must be also highlighted that most

168   of the automatic measurements of geochemical parameters above reported were developed and

169   applied in volcano monitoring, while only recently the geochemical community is moving to apply

170   some of those tracers to seismic monitoring. In terms of hydrogeochemical monitoring, apart the

171   physical-chemical parameters in water (e.g., temperature, water level, electric conductivity, and

172   others such as pH and Eh but with less precision and accuracy) for which automatic sensors exist

173   since long time, the automatic and high-frequency measurement of the water's composition is limited

174   to a few sensors developed in the last decade or so, which mostly focus on the concentration of a few

175   gas species dissolved in waters (e.g., CO_2, CH_4, total gas pressure; De Gregorio et al., 2005,

176   Inguaggiato et al., 2011b). As for gas sensors, most of the automatic measurements of water's

177   composition were developed for volcano monitoring applications.

178   At present, in Italy, hydrogeochemical and geochemical seismic monitoring is limited to

179   selected areas or sites, and it is essentially performed by several departments of INGV in the

180   framework of individual initiative such as the Alto Tiberina Near Fault Observatory (TABOO,

181   https://ingv.it/en/monitoring-and-infrastructure-a/monitoring-networks/the-ingv-and-its-

182   networks/taboo, Chiaraluce et al., 2014) or recent and on-going INGV projects such as the Dynamic

183   Planet (https://progetti.ingv.it/it/pian-din), FURTHER (https://progetti.ingv.it/en/further), MYBURP

184   (https://progetti.ingv.it/it/pian-din#myburp-modulation-of-hydrology-on-stress-buildup-on-the-

185   irpinia-fault), Multiparametric Networks or Rebuilding Central Italy, DL50 and related tasks (e.g.

186   Idro-DEEP CO_2, Idro Calabria, Idro Nord), concerning the groundwater continuous monitoring (e.g.

187   springs and thermal waters) of different areas of mainly Central and Southern Italian Apennines

188   (https://www.pa.ingv.it/index.php/progetti/)   and   Radon   monitoring   (IRON   project,

189   https://ingv.it/monitoraggio-e-infrastrutture/reti-di-monitoraggio/l-ingv-e-le-sue-reti/iron).   In

190   particular, the Alto Tiberina Near Fault Observatory is managed by EPOS (European Plate Observing

191   System) research infrastructure (https://www.epos-eu.org/) of which the mission is to foster the

192   integration of solid earth data and their by-products made by the entire European scientific

193   community: in this case, seismological, geophysical, geodetic and geochemical data recorded by

194   TABOO-Near Fault Observatory are accessible via the FRIDGE European web portal

195   (https://fridge.ingv.it/index.php).

196   Further local monitoring initiatives are provided by other institutions or Universities through

197   the installation of geochemical stations and probes in different parts of the national territory such as

198   in Tuscany, by the IGG-CNR (Institute of Geoscience and Earth Resources,

199   https://www.igg.cnr.it/en), in Southern Italy, by the IMAA CNR (Institute of methodologies for

200   environmental   analysis,   https://www.cnr.it/en/institute/055/institute-of-methodologies-for-

201   environmental-analysis-imaa) or Central Italy, by the Earth Sciences Department (DES,

202   https://www.dst.uniroma1.it/en) of Sapienza University of Rome (Martinelli et al., 2021).

203   Consequently, at a national scale the hydrogeochemical and geochemical monitoring is not

204   organized by using an ad hoc reference institutional database or web portal able to homogeneously

205   archive and distribute high quality multiparametric data to the scientific community. At present and

206   at the best of our knowledge, the only existent databases focus only on mapping gas emissions (e.g.,

207   MaGa, http://www.magadb.net/) or thermal springs, without archiving data from a regular

208   monitoring. A first attempt was recently made in the framework of an agreement between the National

209   Institute of Geophysics and Volcanology (INGV) and the National System for Environmental

210   Protection (SNPA, https://www.snpambiente.it/, comprising the Regional Environmental Protection

211   Agencies, ARPA, and the Italian Institute for Environmental Protection and Research, ISPRA,

212   https://www.isprambiente.gov.it/), with the aim of sharing data from the continuous monitoring of

213   water wells and springs, in particular the piezometric level, temperature, electrical conductivity,

214   salinity and total dissolved solids (Comerci et al., 2019).

215

216   **4 MUDA database**

217

218   MUDA is a dynamic and relational multiparametric database designed and built using a table

219   structure that can correlate data of a different nature (i.e. seismic, hydrogeochemical, geochemical,

220   meteorological). It is adaptable to further types of data from other projects and capable of integrating

221   perfectly with those already acquired via both real time and off-line transmission vectors (Figure 5).

222   The MUDA database is based on MySQL (https://www.mysql.com/it/), a popular and efficient open

223   source relational database management system for handling large amounts of data. Particular attention

224   has been paid to optimising and, above all, integrating all the different types of data taken from

225   different sources while trying to maintain a certain structural uniformity, also open to possible future

226   new implementation.

227   Data collection takes place separately for each type of monitoring station (Table 1), each according

228   to its preferred channels (email, ftp system, Application Programming Interface API, Structured

229   Query Language SQL) in a effort to improve each procedure, avoid data loss and minimise the time

230   taken to receive data.

231   Data are acquired and then archived on a centralised server from which all pre-processing procedures

232   are then carried out to insert this data, after appropriate checks and automatic analysis, into the MUDA

233   database (see next chapter for details). All data downloaded from the remote stations, after the check

234   and processing phase are stored in files before the population of the MySQL database. This is also

235   convenient to have a native and complete data backup, for future requirements.

236   The MUDA database is structured to consider all the different types of monitoring stations at the same

237   multiparametric site through a univocal internal site code, linked to all different types of data. At the

238   same time, however, the independence of the data of each different station is also maintained, as each

239   individual site may have its own particular condition and metadata. For each type of monitoring

240   station, the MUDA database includes 2 tables, one for the station metadata and the other for the

241   recorded data, linked by a unique station id.

242

243   **4.1 Processing of raw data**

244

245   The MUDA project currently includes 5 types of data: hydrogeochemical, meteorological,

246   Radon, CO_2 and seismic. All data are pre-processed to align each time series to the common UTC

247   (Coordinated Universal Time) time. Hydrogeochemical, seismic, meteorological and Radon data are

248   moreover resampled in order to have a representative data each few minutes (i.e. from 1 to 5), namely

249   a good enough interval to see possible cross-correlation signals on different parameters. A data

250   resample is a priori necessary in order to at first homogenize data for viewing and comparison, but

251   also to allow the web page to have a fast response to any query involving long time periods (actually

252   up to a maximum of 30 days) of continuous and high-frequency multiparametric recordings. In

253   particular, while hydrogeochemical, gas and meteorological data are uploaded into MUDA database

254   as raw data with only a consistency check, the seismic data are pre-processed in order to obtain

255   waveforms metadata to be included into MUDA database and to be easily comparable in terms of

256   time series to the other parameters.

257   The processing of raw data for each of the 5 parameters included in MUDA is described in detail in

258   the following.

259   The hydrogeochemical data are acquired by two different type of instrumentation, the first

260   provided by Van Essen Instruments (https://www.vanessen.com/) and the second by STS-Italia S.r.l.

261   (https://www.sts-italia.it/). Data recorded by Van Essen Instruments and STS-Italia are set to sample

262   records every one and ten minutes, respectively. In both cases, groundwater level (m), electrical

263   conductivity (μS/cm), and temperature (C°) are achieved using probes (e.g. CTD-Diver®,

264   https://www.vanessen.com/) installed in correspondence of wells or springs by using weir

265   flowmeters; the recorded chemical and physical parameters are sent at defined time intervals to the

266   remote company head offices and then to the INGV acquisition centre by proprietary API or email.

267   At present, remote stations send data in ASCII format twice a day (i.e. 9 a.m. and 9 p.m., Central

268   European Time, CET) as an email attachment or by ftp-protocol. Depending on the target

269   instrumentation, before populating the MUDA database, a pre-processing is necessary: as an example,

270   the Van Essen probes for water wells need a barometric compensation to account for atmospheric

271   pressure variations in order to provide the corrected water level value (Ferrari et al., 2024). Automatic

272   data acquiring and processing tools have been developed in Python (https://www.python.org/), while

273   automatic tools for populating the MUDA database have been developed in PHP language

274   (https://www.php.net).

275   The meteorological data included in MUDA are provided by Davis Vantage Vue®

276   instrumentation (https://www.davisinstruments.com/). Each single meteorological station, placed

277   near the water well, provides information on atmospheric pressure (mbar), temperature (C°), humidity

278   (%), rainfall amount (mm), wind speed and direction. Also in this case, data take advantage of

279   GPRS/LTE technologies and are gathered by a dedicated WeatherLink Live cloud platform, making

280   them available in real time on the dedicated website (https://www.weatherlink.com/). With samples

281　every one minute, data are archived into the Davis server-cloud and then shared by payment to the

282　end-users (e.g. INGV server) through proprietary Application Programming Interface (API) set into

283　an automated ad-hoc developed python tool, suited for all the different kinds of meteorological

284　instrumentation at each site. Just as for hydrogeochemical data, meteorological parameters are then

285　automatically inserted into the MUDA database twice a day (i.e. 9 a.m. and 9 p.m. CET) using a

286　procedure developed in PHP.

287　　　The Radon data are provided by the IRON network (Italian Radon mOnitoring Network,

288　https://ingv.it/monitoraggio-e-infrastrutture/reti-di-monitoraggio/l-ingv-e-le-sue-reti/iron, Cannelli

289　et al., 2018). Stations, placed next to the water well, measure the concentration of gas in the air using

290　a photodiode detector (AER Plus, Algade), with a sensitivity of 15 Bq/m^3 by counts/hour. Data are

291　measured and acquired every 4 hours together with temperature and humidity, Radon data are

292　transmitted in real time by the Sigfox (https://www.sigfox.com) 0G-technology and archived at the

293　Sigfox cloud, with the exception of particularly remote sites where a periodic local data downloading

294　is also necessary. Radon data are provided in csv format, where the concentration is measured in

295　Bq/m^3, and then uploaded into the MUDA database using an ad-hoc developed PHP tool. In this case,

296　the procedure is manually started after each single data downloading.

297　　　The CO_2 soil flux measurements are acquired using an accumulation chamber provided by

298　Thearen S.r.l (https://thearen.com/). The permanent stations have a no-stationary flux chamber and

299　are equipped with an infrared analyser measuring CO_2 concentrations ($g \cdot m^{-2} \cdot d^{-1}$) in a time frame of

300　three minutes. A single CO_2 flux measure is returned each hour already corrected for pressure (mbar)

301　and temperature (C°) recorded inside the chamber. Soil temperature and humidity (%) and

302　meteorological parameters (atmospheric pressure, temperature, humidity, rain, wind speed and

303　direction) are acquired concurrently. Data are sent to the head company server-cloud through a

304　dedicated modem with automatic data transmission. Data are acquired daily by the INGV acquisition

305　centre through an ad-hoc server to server link using an internal INGV-VPN (Virtual Private Network)

306   connection. Data provided in csv format, are then daily automatically inserted into the MUDA

307   database by using an ad-hoc developed PHP tool.

308   The Seismic data are acquired by selected stations of the Italian National Seismic Network

309   (RSN, https://eida.ingv.it/it/networks/network/IV) and the multiparametric network of Northern Italy

310   (PDnet, https://eida.ingv.it/it/networks/network/ZO) placed near the water well used for

311   hydrogeochemical data. Recorded data are codified following the international standard commonly

312   used by the seismological community, namely the FDSN (https://www.fdsn.org/) network-station

313   code   and   SEED   (Standard   for   the   Exchange   of   Earthquake   Data,

314   http://www.fdsn.org/seed_manual/SEEDManual_V2.4.pdf)   format   supported   by   European

315   Integrated Data Archive, EIDA (https://eida.ingv.it/it/) and maintained by the FDSN. Data are

316   transmitted by different technologies (LTE, satellite, etc.) to the INGV Milano acquisition centre

317   where they are archived through a Seiscomp4 (https://www.seiscomp.de/doc/apps/seedlink.html)

318   client to improve the SeedLink real time data acquisition protocol. Data are archived in the standard

319   binary miniSEED format (http://ds.iris.edu/ds/nodes/dmc/data/formats/miniseed) and organized in a

320   structured archive. Seismic data are pre-processed every night considering the 24 hours of all

321   miniSEED files recorded by stations on the previous day and then checked for quality before being

322   automatically included in the MUDA database by using an ad-hoc developed PHP tool.

323

324   **4.2 Seismic data processing**

325

326   Seismic data collected by MUDA come from permanent and temporary networks able to send

327   data in real time to the INGV acquisition centres. Following the international standard shared among

328   the seismological community, continuous data streams are usually archived in miniSEED format.

329   Depending on the adopted sampling rate, usually 100 Hz for seismometers and 200 Hz for

330   accelerometers, the amount of data per day relative to a single component data stream of motion at

331   one station ranges between about 6 and 10 Mbyte/day for seismometers and between 15 and 20

332 Mbyte/day for accelerometers. Multiplying this amount of data by a large number of stations, the

333 result is a daily amount of data that easily increases in the order of Gbytes and that is not easy to

334 manage in the framework of an immediate distribution provided by a thematic web portal.

335 Considering the main goal of MUDA, namely a daily dynamic updating web portal, for comparing

336 and downloading all multiparametric real time continuous data, and also considering the sampling

337 rate of the other available instrumentation (i.e. spanning from one record per minute to one record

338 every four hours), the continuous seismic data streams are processed in order to conform the contents

339 to the web portal requirements before inclusion in the MUDA database.

340 Seismic data are acquired and stored following the standard Seiscomp archive structure. Every night

341 at 2 a.m. miniSEED files relative to the 24-hour recordings of the previous day are selected at each

342 station and processed by using an ad-hoc procedure developed by merging the Bash and SAC

343 (Seismic Analysis Code, https://ds.iris.edu/files/sac-manual/) scripting languages.

344 The processing scheme starts by downloading at each single recording station 24 hours of miniSEED

345 files; data are then separated into 288 sub-windows, each one with length of 5 minutes starting from

346 the origin time of each single miniSEED file (usually corresponding to the 00:00:00 UTC if the station

347 works well). Then, for each 5-minute windows, raw data recorded in counts are converted to the

348 proper unit of measurements (cm/s for seismometers and gal for accelerometers) and the sensor

349 response curves are removed by deconvolution and finally filtered using a 4th order Butterworth filter

350 in the range 0.1 - 20 Hz. For each single sub-window relative to a specific channel recorded by a

351 specific station, the RSM (Root Mean Square, e.g. Goldstain et al., 2003), the maximum ground

352 shaking in terms of velocity (cm/s), the mean amplitude value of the whole FFT (cm/s/Hz) (Fast

353 Fourier Transform, e.g. Bormann 2012) and the maximum amplitude of the FFT for frequency

354 interval spanning from 0.1 Hz to 20 Hz, are calculated, providing for each parameter 288 values per

355 day, corresponding to the daily upload of hydrogeochemical and meteorological data. In particular,

356 the Root Mean Square is calculated for the entire time windows using the following equation:

357

358        $$x_{RMS} = \sqrt{[1/n\ (x1^2 + x2^2 + \dots + xn^2\ )]} \qquad (1)$$

359

360   where x is the amplitude of the single sample, and n the number of samples of the trace considered.

361   Daily time series of RMS, PGV, FFT-mean and FFT(f) are finally uploaded into the MUDA database

362   using an ad-hoc developed PHP tool.

363
364
365   **4.3 Data availability and dissemination**

366

367   MUDA publishes and shares the available data recorded at each site through a specific web

368   interface developed in PHP (https://www.php.net/) to easily and effectively interact with MUDA SQL

369   database, and using a responsive design in HTML5, capable of adapting automatically to any device

370   on which it is displayed (i.e. PC, tablet, smartphone, etc.). As a final step, the data publication required

371   assigning a regular DOI associated to the DB and provided by INGV data management office through

372   a standard procedure. The final DOI of MUDA is https://doi.org/10.13127/SD/ku7Xm12Yy9. Data

373   have been licensed using the Creative Commons License CC BY 4.0. MUDA web portal publishes

374   multiparameter data daily and updated to the previous day. It offers the chance to view and download

375   dynamic time series for all available data and for different time periods, up to a maximum of 30 days.

376   In reference to longer periods, an e-mail request can be sent to: muda@ingv.it.

377   The web portal has a main page showing an interactive map of Northern and Central Italy, as

378   at present MUDA acquires data from automatic stations located in this part of the Country, where the

379   multiparametric stations are indicated by triangles with pop-ups showing the main features (i.e.

380   coordinates and available instrumentation) of the target site, including the direct access to the dynamic

381   data viewing (Figure 3) and to the single station page (Figure 4). The home page on the top right

382   corner shows a pop-up menu with selectable thematic layers including the reference seismic hazard

383   map of the national territory in terms of peak ground acceleration (MPS04 working group,

384   http://zonesismiche.mi.ingv.it/, Stucchi et al., 2011), the seismogenic areas and the active faults taken

385   from the Database of Individual Seismogenic Sources database (DISS, https://diss.ingv.it/, DISS

386   working group 2021), recent (https://terremoti.ingv.it/) and historical

387   (https://emidius.mi.ingv.it/CPTI15-DBMI15/) seismicity bulletins, and the location of seismic

388   stations of the National Seismic Network (RSN, https://eida.ingv.it/it/networks/network/IV) managed

389   by INGV.

390   The *View & Download DATA* web page, accessible from the horizontal tool bar of the home

391   page, opens the dynamic data viewing (Figure 3). Users can select for each multiparameter site the

392   time series to be displayed backwards in time (i.e. 1 day, 7 days, 15 days, 30 days) starting from a

393   selected date. Once the site and period have been chosen, the available data automatically appear

394   synchronised with respect to UTC (Coordinated Universal Time). From top to bottom, these are:

395   hydrogeochemical data from well or spring sensors showing water temperature (°C), electrical

396   conductivity (µS/cm) and the value of the water column (m) above the sensors; meteorological data

397   showing air temperature (°C) and rainfall (mm); seismometric data showing the Root Mean Square

398   (RMS), the maximum ground velocity values (cm/s), the average Fourier spectrum (FFT) amplitude

399   values, the Fourier spectrum values for frequency bands selected in the interval 0.1 - 20 Hz; Radon

400   gas emissions (Bq/m^3) and soil CO_2 flux ($g \cdot m^{-2} \cdot d^{-1}$). All interactive graphs can be zoomed with the

401   left mouse button and they enable selecting individual functions using pop-up layers. In each graph,

402   in the top right-hand corner, it is possible to view the individual image in full screen and download

403   the selected data in csv (Comma Separated Values) format as well as the images in pdf (Portable

404   Document Format), png (Portable Network Graphic), jpeg (Joint Photographic Experts Group), svg

405   (Scalable Vector Graphics) formats. The last selectable item, on the right of this page, gives the

406   possibility of viewing a single parameter, for a more detailed observation.

407   A further topic of the MUDA web portal is the single station web page (i.e. link *STATIONS*),

408   also reachable from the horizontal tool bar. This web page is designed to provide a first and general

409   geophysical and geochemical characterization of each multiparametric site. In particular, each single

410   station web page shows, on the left, a thematic map indicating the location of the monitoring site.

411   Below the map, the two links provide a geological and morphological setting of the area. For each

412   recording site, a portion selected from the geological map at a 1:100,000 scale (Società Geologica

413   Italiana, http://www.isprambiente.gov.it/it/cartografia/) is provided, with topographic base at

414   1:25,000   scale   (Istituto   Geografico   Militare,

415   http://www.igmi.org/prodotti/cartografia/carte_topografiche/). Concerning morphology, for each

416   recording site, a topographic map (i.e. Slope and Ridge) is proposed by considering the available

417   digital   elevation   model   (ASTER   GDEM   with   a   cell   size   of   10   m,

418   https://www.earthdata.nasa.gov/news/new-aster-gdem). Starting from the processed DEM, the slope

419   map was constructed with three topographic classes (0°–15°, 15°-30°, and >30°), considering the

420   break values defined in the current Italian seismic code (NTC, 2018). The ridgelines were extracted

421   using the Topographic Position Index (TPI) algorithm (Weiss, 2001; Pessina and Fiorini, 2014). On

422   the right, the web page shows thematic tables relative to the installed instrumentation. At each site,

423   besides the general information on coordinates and technical features of the instruments, a

424   geophysical characterization of the site is also provided in terms of polarized horizontal to vertical

425   spectral ratio (HVSR) and each single log performed in the wells regarding water electrical

426   conductivity and temperature as a function of the available stratigraphy together with the main

427   features of monitored well or spring. Finally, in each station web page, graphs relative to the whole

428   hydrogeochemical time series are also downloadable.

429

430   **5 Data Records**

431

432   At present (i.e. 31 March, 2024), MUDA includes data from 25 multiparametric sites (Table

433   1) located in Northern and Central Italy (Figure 2), both already monitored by permanent INGV

434   infrastructures or installed in the framework of recent INGV research projects. It is worth mentioning

435   that not all multiparametric sites are characterized by homogeneous multiparametric instrumentation

436   (Figure 6). In any case, all available data are always sent in real time to the INGV acquisition centres.

437   In particular, concerning seismic data, the multiparametric sites include 7 stations belonging to the

438   permanent National Seismic Network (RSN, https://eida.ingv.it/it/networks/network/IV) and 12

439   stations belonging to the temporary multiparametric network of Northern Italy (PDnet, FDSN code

440   ZO, https://eida.ingv.it/it/networks/network/ZO), installed in the framework of the INGV Dynamic

441   Planet S2-project. These sites are located in Northern Italy, around the Lake Garda, at the southern

442   limit of the Eastern Italian Alps and in the central portion of the Po Plain (Figure 2). A further 2

443   seismic stations (PDN11, PDN12, table 1) have recently been installed in the framework of the INGV

444   Dynamic Planet GEMME (Integrated Geological, gEophysical and geocheMical approaches for 3D

445   Modelling of complex seismic site Effects) project, in Norcia basin (Apennine chain in central Italy)

446   and its surroundings (Figure 2). Finally, one seismic station (PDN10, table 1) has been installed in

447   cooperation with the Dynamic Planet PROMUD (Definition of a multidisciplinary monitoring

448   PROtocol for MUD volcanoes) project, in the Salse di Nirano Reserve (Italian Northern Apennines,

449   Figure 2).

450   In general, seismic stations are equipped with high dynamic 24-bit digital recording systems

451   coupled to enlarged (5s owner period) or broadband (120s owner period) seismometers. In particular,

452   at Oppeano multiparametric site (Table 1), borehole instrumentation is installed at 150 m depth. Even

453   if in some cases accelerometer sensors are coupled to the target seismmometer (velocimeter), MUDA

454   includes only seismmometric data due to their higher sensitivity and best resolution with respect to

455   possible occurrences of natural phenomena such as micro seismicity, local weak motion earthquake

456   occurrences and/or teleseisms or environmental modifications (i.e. landslides, low atmospheric

457   pressure, tides etc.).

458   Hydrogeochemical data are recorded in all 25 multiparametric sites (Table 1), at both wells

459   and springs set up in the framework of INGV Dynamic Planet projects (S2 and GEMME) and INGV

460   Multiparametric Networks or the Rebuilt central Italy, DL50 project. The Toppo site (Table 1),

461   installed in the eastern Alps in the framework of the Eccsel Eric consortium

462   (https://www.eccsel.org/), is managed by OGS (National Institute of Oceanography and Applied

463   geophysics, https://www.ogs.it/en) in cooperation with the University of Ferrara (Department of

464   Physics and Earth Science, http://fst.unife.it/en) and the INGV. At present, data included in MUDA

465   are recorded at 22 wells and 3 springs (Recoaro, Recoaro1, Feltre, see table 2). In general, wells have

466   depths ranging from a few meters (< 10 m) to a maximum of 300 m for Toppo and Mirandola sites

467   (Table 2). The instrumented wells have a mean depth between 5 and 150 m. In particular, the

468   monitored well named TRIPONZO (Table 2) is characterized by the presence of thermal waters.

469   All sites monitored by hydrogeochemical instrumentation are also equipped with a

470   meteorological station able to capture the main atmospheric variations.

471   Four sites (i.e. Montelungo, Bondo, Norcia, Triponzo, table 1) are currently equipped with

472   instrumentation able to record the Radon concentration in the air. Sensors for Radon monitoring are

473   part of the IRON network (Italian Radon mOnitoring Network, https://ingv.it/monitoraggio-e-

474   infrastrutture/reti-di-monitoraggio/l-ingv-e-le-sue-reti/iron) of INGV. Finally, just one site (i.e.

475   Nirano, table 1) is equipped with instrumentation for Carbon Dioxide (CO_2) soil flux measurements.

476   In general, the multiparametric sites show co-located instrumentation, with a few exceptions

477   due to logistic difficulties during the site installation or other technical problems (e.g. sites with a

478   very high level of background seismic ambient noise or working pump installed in well). In all cases,

479   the reference seismic station is installed in the same geological, morphological and hydrogeological

480   context as the other instruments, possibly co-located or at least in the proximity. Hydrogeochemical

481   stations installed in a narrow area (e.g., Bulgarelli, Medolla, Mirandola and Secchia sites, table 2)

482   might refer to the same seismic station.

483

484   **5.1 Data quality check**

485

486   In order to verify the completeness and correctness of the recorded data, we carried out several

487   checks.

488   Concerning seismic data included in MUDA, the results of the processing procedure to

489   produce 5 minutes interval data are verified to check the capacity of the proposed processing scheme

490   to represent a real marker to detect earthquakes or environmental phenomena. Figure 7 reports an

491   exhaustive example at the Oppeano site for events recorded by the seismic station on December, 29,

492   2020. Figure 7 shows in the panel *a* (top) the occurrences of subsequent events in a narrow time

493   window spanning from 2020-12-29 14:02:40 to 15:36:57 UTC. The first evident transient is related

494   to the regional M_w=6.3 Croatia earthquake on 2020-12-29 at 12:19:54 UTC

495   (https://terremoti.ingv.it/event/25870121). A few hours later, a small sequence of three local weak

496   motion was recorded 12 km South West of Oppeano and localised by the INGV bulletin at 2020/12/19

497   14:02:40, 14:44:51 and 15:36:47 UTC with magnitudes of M_L=3.4, M_L=2.8 and M_w=3.9, respectively

498   (https://terremoti.ingv.it/event/25871441). In the bottom of panel *a* the results of our detector

499   procedure in terms of FFT interval is shown for the 288 data points of the 2020/12/29. It is evident

500   how all transients have been clearly recognized by marked peaks: in particular, the regional event,

501   occurring about 400 km East of the Oppeano well highlights a notable contribution at low frequency,

502   showing a clear peak for the FFT around 0.1 Hz. On the contrary, the local seismicity is well described

503   by peaks detected at higher frequency content, in particular ranging from 1 to 10 Hz. In this case, it

504   is worth noting how the high frequency content of FFTs also highlight variations in ambient noise

505   level between night and day. In the panel *b* of figure 7, the results of the detection procedure are

506   presented in terms of relative RSM, ground motion velocity and averaged FFTs (from top to bottom).

507   In order to publish reliable results, all continuous seismic data streams for all seismic stations

508   are checked daily for quality by the interoperability between MUDA and ISMDq (INGV Strong

509   Motion Data quality, http://ismd.mi.ingv.it, Massa et al., 2022). In this way all seismic stations

510   included in MUDA are checked for gaps (%), availability (%) and ambient noise level variation in

511   terms of PSD (Power Spectral Density) and PDF (Probability Density Function), in dB, as calculated

512   by McNamara and Buland (2004). Through ISMDq, it is possible to build temporal time series with

513   a maximum time length of up to 2 years for all stations included in MUDA in order to check at first

514   the correct functioning of the stations, the accuracy of used metadata, daily and seasonal variations

515   of ambient noise level and transient or permanent anthropic disturbances. In particular, in case of

516   failure in data transmission, the continuous monitoring of data gaps and availability allow us to

517   retrieve data directly from station memories thereby avoiding important gaps in the data.

518   Hydrogeochemical and geochemical data are checked daily for availability and gaps usually

519   due to a temporary lack of data transmission platforms (i.e. cellular line or satellite), in particular

520   during rainy and stormy days or more rarely due to malfunctioning of the instrumentation. In the first

521   case, the recorders, thanks to their internal memory and datalogging capacity, are able to archive data

522   up to a maximum of 30 days. If needed, the recovery of data is possible through a manual download.

523   Subsequently data are uploaded into the MUDA database by calling the same ad-hoc developed tools

524   for populating the database for each parameter, with appropriate flags. In some cases, water level time

525   series show unusual abrupt peaks (spikes) due to some problem during the compensation of

526   atmospheric pressure performed by the recording system in order to obtain the correct values of water

527   level: in general, misalignments in pressure compensation lead to wrong water level values, usually

528   with differences of ~ 10 m, as a consequence of the measured atmospheric pressure usually around

529   or slightly above 1000 mbar, considering that all the stations are within a few hundred meters above

530   sea level.

531   Other data included in MUDA (i.e. meteorological, Radon, CO_2 flux) do not need particular

532   processing. In any case, for all meteorological, Radon and CO_2 measurements, data are always

533   checked for gaps and possible spurious peaks that should be deleted. In particular, meteorological

534   data regarding the pluviometry are archived and uploaded into MUDA as a single sample recorded

535   each minute, or even better, in some cases, at each individual movement of the rain gauge's tipping

536   bucket (0.2 mm every time). In these cases, before publishing the rain values on the web site, data are

537   cumulated in intervals of 1 hour directly in the SQL query made by the web portal, in order to better

538   highlight heavy storms or other particular meteorological phenomena.

539

6 Multiparametric monitoring

540

541

542   In this session, some examples of comparison among multiparametric data are presented and

543   discussed in the framework of their possible applications for research and services devoted to natural

544   hazard risk reduction.

545   An interesting example of multiparametric monitoring, concerning groundwater level

546   variation presumably related to a large landslide phenomena has been collected at the Bondo (Table

547   1) site and aquifer (Lake Garda area, Figure 2), where on the November 1, 2023, the water column

548   above the sensor in the well abruptly increased by ~ 20 m. This significant modification, also

549   combined with the diminishing temperature and electrical conductivity (Figure 8, panel *a*), happened

550   as a consequence of 2 days of intense rainfall with measured values of precipitation in a narrow area

551   surrounding Bondo up to 400 mm. It is important to highlight that the stratigraphy below Bondo is

552   mostly made of fractured-carsified limestones belonging to the Dolomia Principale formation (Upper

553   Triassic). To explain such a notable groundwater level variation, additional and contemporary natural

554   phenomena should be hypothesized; on the basis of the information provided by the local media, in

555   the same period the area was affected by diffuse landslides. In particular, between October 31 and

556   November 1, 2023, a clear seismic transient (Figure 8, panel *b*) was recorded on all 3 components of

557   ZO.PDN3 station (Table 2), characterized by very long duration (i.e. some hours), higher amplitudes

558   with respect to the local ambient noise level (i.e. the Peak Ground Velocity, PGV was equal to 0.01

559   cm/s, comparable to a local earthquake with magnitude ranging from 2.5 and 3.0), prevalent high

560   frequency content (~ 5-30 Hz) and a strong polarisation with preferential amplification of motion

561   along the NS direction (Figure 8, panel *c*). In this case, the recorded transient at ZO.PDN3 could in

562   fact be attributable to local and diffuse landslides that could have modified the volume and/or the

563   extent of the aquifer and eventually the water flow infiltration and circulation through the rock

564   fractures by influencing the water level and leading the aquifer to be more sensitive to meteorological

565   events.

566   Meteorological events, in particular the intense rainfall period, also seem to have a strong

567   influence on Radon emission measurements, usually adopted as a possible marker in case of a tectonic

568   event. An example can be observed considering the complete Radon time series at the Bondo site

569   where data highlight a positive correlation with the seasonality, with increasing values in summer and

570   decreasing values in winter, following the trend of both atmospheric pressure and temperature. At

571   least during the monitored period, at the Bondo site no correlation with local seismicity appears to be

572   noticeable, while clear correlations between Radon outliers and the rainfall period are evident (Figure

573   9, panel *a*). It is worth mentioning how not all Radon sensors show the same behaviour with respect

574   to the season. At the Montelungo site (Table 1), for instance, data show a complete anti-correlation

575   with the seasons (Figure 9, panel *b*), with lower values in summer and higher values in winter,

576   probably as a consequence of the different local geological and morphological setting.

577   A further example regards the CO_2 flux variation, measured at the Nirano site (Table 1) in

578   October 2023 (Figure 10, panel *a*) during an intense period of weak motion earthquakes localized

579   very close to ZO.PDN10 station, installed in the area of the Salse di Nirano regional park. Starting

580   from June 2023, the area of Nirano showed an increase in the local seismicity. In the period

581   2023/06/01 to 2023/11/15, 32 earthquakes with local magnitude (M_L) in the range 2.0-3.5 were

582   recorded with a maximum epicentral distance from Nirano of 30 km. In particular, the strong events

583   with M_L=3.5 occurred on 30th October 2023 (04:25:53 UTC). Considering the CO_2 time series

584   recorded at Nirano, and a time period spanning from October 15th to November 15th, it is possible to

585   highlight the presence of many CO_2 data points with values exceeding the limit of +1 standard

586   deviation (Figure 10, panel *b*), with respect to the average values of the period. Many outliers were

587   recorded just before and also soon after the M_L=3.5 target earthquake. It worth noting that this

588   evidence should be carefully evaluated also considering other parameters (for instance, atmospheric

589   pressure, soil moisture and temperature), even though no relevant rainfall episodes occurred in that

590   period.

591   Further case studies concern the correlation between meteorological (i.e. temperature and

592   rainfall) and groundwater parameters. Understanding water level fluctuation patterns is one of the

593   pillars for designing adaptive management practices that can mitigate the impacts of extreme water

594   levels on infrastructure and associated economic activities (e.g. Gerten et al., 2013, Alley et al., 2002,

595   Taylor et al., 2009; Russo and Lall, 2017). Groundwater recharge is difficult to estimate, especially

596   in fractured aquifers, because of the spatial variability of the soil properties and because of the lack

597   of data at basin scale. A possible solution consists in inferring recharge directly from the observation

598   in boreholes (Guillaumot et al., 2022), even if the direct measures in wells overlook the impact of

599   lateral groundwater redistribution in the aquifer. When evaluating the effect of exogenous parameters

600   on groundwaters, rainfall is the main factor in promptly influencing all monitored groundwater

601   parameters (e.g. Mancini et al., 2022, Guillaumot et al., 2022), with a variable aquifer response with

602   respect comparable amounts of precipitation in the same period. Figure 11 shows an example of

603   groundwater recordings related to the meteorological event of October 2023 at Volargne and Fonte

604   sites (table 1). It is worth noting how in the first site (Figure 11, panel *a*) a gradual and moderate rise

605   in water level is contrasted by a faster and larger (less than 2 hours) increase in water level at the

606   Fonte site (Figure 11, panel *b*), which shows an intense influence of the rainfall, also proved by the

607   extremely variable temperature and conductivity records not observed in the other sites (Ferrari et al.,

608   2024). The light grey box in Figure 11 highlights another instant response of Fonte groundwater to

609   precipitation which is even more sharper than the one described above and also involves electrical

610   conductivity decrease and temperature increase.

611   The atmospheric temperature is moreover proven to affect groundwater temperature,

612   especially in aquifers down to ~ 20 m depth (e.g. Lee and Hahn, 2006, 2021; Taylor and Stefan, 2009;

613   Menberg et al., 2014). Monitoring sites having at least 1 year of recordings are taken into account to

614   analyse groundwater temperature seasonal oscillations and correlations to air temperature. In our

615   case, the absence of seasonality is detected at the Bondo, Montelungo and Volargne sites (Table 1)

616   where the constant groundwater temperatures could be explained by the aquifer depth (~ 50 m). In

617   other cases, such as the Casaglia site (Table 1), despite the depth of aquifer of a few meters below

618   ground level, the relevant water (~ 40 m) column above the hydrogeochemical sensor dampened

619   possible temperature fluctuations (Bucci et al., 2020; Egidio et al., 2022). On the contrary, at the

620   Balconi site (Table1), despite the aquifer depth is greater than 50 m, a nearly seasonal variation

621   characterized by maximum values reached in summer and minima in winter, is observed, in

622   agreement with the measured air temperature periodicity (Ferrari et al., 2024). However, it should be

623   evaluated whether this temperature variation in specific seasons is directly attributable to

624   meteorological reasons or to anthropogenic causes, due to intense irrigation occurring in the area of

625   Balconi during the most dry and hot months of the year.

626

627   **7 Data Availability**

628

629   Data and metadata presented and described in this manuscript can be accessed

630   under https://doi.org/10.13127/muda (Massa et al., 2023).

631

632   **8 Usage Notes and conclusions**

633

634   The technical validation allowed us to obtain a reliable and homogenous dataset of continuous

635   multiparametric time series and associated metadata. For hydrogeochemical, meteorological, Radon

636   and CO_2, data are published in a raw format after a pre-processing whose main scope was just to

637   detect gaps and spurious peaks to be deleted from the time series. Seismic data are published after

638   applying a 5-minute resampling to the raw miniseed 24-hour continuous data and then by converting

639   the velocity ground motion (cm/s) in RMS and FFT discrete time series. The raw seismic waveforms

640   are however downloadable from the EIDA-Italia webservice (https://eida.ingv.it/it/).

641   For the first time, at least in Italy, high frequency and continuous multiparametric data are

642   dynamically updated daily and published soon after for end users. Data can be used for different

643   purposes, ranging from i) information regarding environmental and meteorological temporal trends

644   with respect the global climate change problematic; ii) details on local aquifers features and

645   seismicity; iii) recommendations for the civil protection; iv) multiparametric geophysical,

646   environmental and geochemical data for research studies. In particular, all seismic stations included

647   in MUDA-db with code ZO (PDnet, https://eida.ingv.it/it/networks/network/ZO) contribute with the

648   national seismic monitoring by sharing a continuous data stream in real time to the INGV National

649   Seismic Network (https://eida.ingv.it/it/networks/network/IV). In particular, the dense ZO network

650   installed around Lake Garda contribute significantly to improving the minimum magnitude threshold

651   detection of the area as reported in Ferrari et al. (2024).

652   Seismic data, together with all geological, morphological and geophysical information

653   collected at each site included in MUDA, can moreover be used to investigate the site response in

654   terms of seismic amplification, in particular for sites installed in the central part of the Po Plain, a

655   deep basin characterized by a significant thickness of incoherent alluvial deposits. Seismic events

656   recorded at each station can also be used for local investigations into the micro seismicity of the area,

657   seismic source recognition or to improve the available seismic velocity models at a local scale.

658   Hydrogeochemical and geochemical data will be used in the framework of a recent agreement

659   between the National Institute of Geophysics and Volcanology (INGV) and the National System for

660   Environmental Protection (SNPA, comprising the Regional Environmental Protection Agencies -

661   ARPA and ISPRA), aimed at gathering information on seismic activity and aquifer/spring status from

662   various acquisition sources, in some cases reaching a near real time monitoring through the SINAnet

663   facility (https://www.snpambiente.it/attivita/sistema-informativo-nazionale-ambientale/).

664   In general, the multiparametric monitoring is the basis by which to understand and identify

665   possible seismic precursors, an objective not yet achieved in earthquake studies. In particular, the

666   short-term earthquake forecasting, remains elusive and largely unattained. An effective solution for

667   such a major issue might be found, in the future, in systematic high frequency and continuous

668   measurements with multiparametric networks operating over the long term. Owing to the influx from

669 deep crustal fluids in active tectonic areas, groundwater monitoring may especially be considered a

670 fundamental tool for investigating pre-seismic signals of rocks undergoing accelerated strain (e.g.

671 King, 1986; Skelton, A. et al. 2014, Barberio et al., 2017).

672

673 **9 Code Availability**

674

675 All the procedures to acquire and process data coming from multiparametric remote stations

676 have been specifically developed for the MUDA project in Bash scripting language, Python and PHP

677 language, using, when necessary, proprietary API taken from the manufacturers of the installed

678 remote instrumentation, as detailed in the text. Seismic data are acquired and archived through a

679 Seiscomp4 (https://www.seiscomp.de/doc/apps/seedlink.html) client, thereby improving the

680 SeedLink real time data acquisition protocol. Some processing steps on the seismic data are

681 undertaken using the Seismic Analysis Code (SAC,

682 https://ds.iris.edu/ds/nodes/dmc/software/downloads/sac/), a software designed for both real time and

683 off-line seismological analyses of time series data. The MUDA database is developed with MySQL

684 open source software. The MUDA web portal is developed in PHP and HTML5 languages, and all

685 data are published under the Creative Commons License CC BY 4.0 licence.

686

687 **Team list**

688

689 MUDA working group is at present composed by the main authors and:

690 Marino Domenico Barberio [4], Rodolfo Puglia [1], Santi Mirenna [1], Ezio D'Alema [1], Anna Figlioli

691 [1], Fabio Varchetta [1], Antonio Piersanti [4], Valentina Cannelli [4], Gianfranco Galli G. [4], Gianfranco

692 Tamburello [5], Gioia Capelli Ghioldi [5]

693

694 [1] National Institute of Geophysics and Volcanology (INGV), Milano department, Italy

695   [(4)] National Institute of Geophysics and Volcanology (INGV), Roma1 department, Roma, Italy

696   [(5)] National Institute of Geophysics and Volcanology (INGV), Bologna department, Italy

697

698   **Author contributions**

699

700   This study started from an original idea by MM and ALR. MM, ALR, EF and SL contributed

701   to all phases of site installations, data acquisition, processing and archiving. DS developed MySQL-

702   Db and the associated web page, as well as the procedures to upload data into MUDA-db. SL and EF

703   contributed to organising the technical data sheet related to each multiparametric site now available

704   at each single station web page. MM developed the procedures for multiparametric data pre-

705   processing and seismic data post processing. All authors participated in the preparation of the

706   manuscript draft.

707

708   **Competing Interests: The authors declare no competing interests.**

709

710   **Acknowledgements**

711

712   We would like to thank all those who contributed to the site search phase and the installation

713   of the PDnet network. In particular: Prof. Tullia Bonomi (Milano Bicocca University), Engr. Michela

714   Biasibetti and Engr. Bruno Pannuzzo (Acque Bresciane company), Engr. Massimo Carmagnani and

715   Engr. Ignazio Leone (Acque Veronesi company), Engr. Giovanni Lepore and Fabrizio Brunello

716   (Azienda Gardesana Servizi company), Engr. Paolo Pizzaia (Alto Trevigiano Servizi company), Arch.

717   Luca Bertanza (municipality of Tremosine Garda, BS), Arch. Umberto Minuta (municipality of

718   Dolcè, VR), Geom. Elena Beraldini (municipality of Negrar, VR), Dr. Marzia Conventi (municipality

719   of Fiorano Modenese, MO - Dir. Riserva Salse di Nirano), Mr. Salviani (Norcia), Bagni Triponzo

720   Terme S.p.A. (municipality of Cerreto di Spoleto), Dr. Luca Martelli and Dr. Paolo Severi (Emilia

Earth System
Science
Data

Open Access

Discussions

721   Romagna Region). Particular thanks go to OGS (National Institute of Oceanography and Applied

722   geophysics, https://www.ogs.it/en) and University of Ferrara (Department of Physics and Earth

723   Science, http://fst.unife.it/en) for sharing data recorded at the TOPPO site in the framework of the

724   ECCSEL-ERIC (European Research Infrastructure for CO_2 Capture, Utilisation, Transport and

725   Storage (CCUS), https://www.eccsel.org/) consortium.

726   The production of the seismic data published in the MUDA database involves many INGV colleagues

727   covering different tasks in the data production chain, from the correct operation of the seismic stations

728   to data acquisition, data processing, archiving and subsequent distribution. We would like to thank all

729   the colleagues of the INGV sections and offices who contribute daily to the management of the

730   National Seismic Network (RSN, https://eida.ingv.it/it/networks/network/IV), as well as providing

731   access to the data they produce.

732

733   **References**

734

735   Aiuppa, A., Federico, C., Giudice, G., Gurrieri, S. Chemical mapping of a fumarolic field: La Fossa

736   Crater, Vulcano Island (Aeolian Islands, Italy). Geophys. Res. Lett. 32 (13), 1-4 (2005).

737

738   Allard, P., Burton, M., Murè F., Spectroscopic evidence for a lava fountain driven by previously

739   accumulated magmatic gas. Nature 433, 407-410, doi:10.1038/nature03246 (2005).

740

741   Alley, W.M., Healy, R.W., LaBaugh, J.W., Reilly, T.E., Flow and storage in groundwater systems.

742   Science 296 (5575), 1985-90, doi: 10.1126/science.1067123 (2002).

743

744   Barberio, M.D., Barbieri, M., Billi, A., Doglioni, C., Petitta, M., Hydrogeochemical changes before

745   and during the 2016 Amatrice Norcia seismic sequence (central Italy). Sci. Rep. UK 7:11735, 1-12.

746   doi:10.1038/s41598-017-11990-8 (2017).

747

748 Battaglia, M., Murray, M.H., Serpelloni, E., Bürgmann, R., The Adriatic region: an in dependent

749 microplate within the Africa-Eurasia collision zone. Geophys. Res. Lett. 31, L09605,

750 doi:10.1029/2004GL019723 (2004).

751

752 Bigi, G., Costantino, D., Parotto, M., Sartori, R., Scandone, P., Structural Model of Italy. Firenze,

753 Società Elaborazioni Cartografiche (S.EL.CA.). Consiglio Nazionale Delle Ricerche Progetto

754 Finalizzato Geodinamica, Scala 1:500.000, 9 Fogli (1990).

755

756 Bonini, M., Elliptical mud volcano caldera as stress indicator in an active compressional setting

757 (Nirano, Pede-Apennine margin, northern Italy). Geology 36, 131-134, doi:10.1130/G24158A.1

758 (2008).

759

760 Bormann, P., (Editor) New manual of seismological observatory practice (NMSOP-2), IASPEI, GFZ

761 German Research Centre for Geosciences, Potsdam, https://gfzpublic.gfz-potsdam.de/ (see data and

762 resources), doi:10.2312/GFZ.NMSOP-2 (2012).

763

764 Bräuer, K., Kämpf, H., Strauch, G., Weise, S.M., Isotopic evidence (^{3}He/^{4}He, ^{13}C$_{CO2}$) of fluid-

765 triggered intraplate seismicity. J. Geophys. Res. 108(B2), 1-11, doi:10.1029/2002JB002077 (2003).

766

767 Brozzetti, F., Lavecchia, G., Seismicity and related extensional stress field: the case of the Norcia

768 Seismic Zone (Central Italy). Annales Tectonicae 8 (1), 36-57 (1994).

769

770 Bucci, A., Lasagna, M., De Luca, D.A., Acquaotta, F., Barbero, D., Fratianni, S., Time series analysis

771 of underground temperature and evaluation of thermal properties in a test site of the Po plain (NW

772 Italy). Environ. Earth Sci. 79,185, doi:10.1007/s12665-020-08920-9 (2020).

773

774   Burton, M.R., Caltabiano, T., Murè, F., Salerno, G.G., Randazzo, D., SO2 flux from Stromboli during

775   the 2007 eruption: results from the FLAME network and traverse measurements. J. Volcanol.

776   Geotherm. Res. doi:10.1016/j.jvolgeores.2008.11.025 (2009).

777

778   Burrato, P., Vannoli, P., Fracassi, U., Basili, R., Valensise, G., Is blind faulting truly invisible?

779   Tectonic-controlled drainage evolution in the epicentral area of the May 2012, Emilia-Romagna

780   earthquake sequence (northern Italy). Annals of Geophysics 55, 4, 525-531 (2012).

781

782   Buttitta, D., Caracausi, A., Chiaraluce, L., Favara, R., Morticelli, M.G., Sulli, A., Continental

783   degassing of helium in an active tectonic setting (northern Italy): the role of seismicity. Scientific

784   Reports 10, Article number:162 (2020).

785

786   Cannelli, V., Piersanti, A., Galli, G., Melini, D., Italian Radon mOnitoring Network (IRON): A

787   permanent network for near real-time monitoring of soil radon emission in Italy. Annals of geophysics

788   4/61, 10.4401/ag-7604 (2018).

789

790   Carapezza, M.L, Inguaggiato, S., Brusca, L., Longo, M., Geochemical precursors of Stromboli 2002–

791   2003 eruptive events. Geophys Res Lett 31(7):10.1029/2004GL019614 (2004).

792

793   Castaldini, D., Valdati, J., Ilies, D.C., Chiriac, C., Bertogna, I., Geo-tourist map of the natural reserve

794   of Salse di Nirano (Modena Apennines, Northern Italy). Italian Journal of Quaternary Sciences 18(1),

795   245-255 (2005).

796

797   Cicerone, R.D., Ebel, J.E., Britton, J., A systematic compilation of earthquake precursors.

798   Tectonophysics 476, 371-396, doi:10.1016/j.tecto.2009.06.008 (2009).

799

800   Chiarabba, C., Piccinini, D., De Gori, P., Velocity and attenuation tomography of the Umbria Marche

801   1997 fault system: Evidence of a fluid-governed seismic sequence. Tectonophysics 476, 73-84,

802   doi:10.1016/j.tecto.2009.04.004 (2009).

803

804   Chiaraluce, L., Collettini, C., Cattaneo, M., Monachesi, G., The shallow boreholes at The

805   AltotiBerina near fault Observatory (TABOO; northern Apennines of Italy), Volume 17, Scientific

806   Drilling, 17, 31-35, https://doi.org/10.5194/sd-17-31-2014 (2014).

807

808   Chiaraluce, L., Di Stefano, R., Tinti, E., Scognamiglio, L., Michele, M., Casarotti, E., Cattaneo, M.,

809   De Gori, P., Chiarabba, C., Monachesi, G., Lombardi, A., Valoroso, L., Latorre, D., Marzorati, S.

810   The 2016 Central Italy Seismic Sequence: A First Look at the Mainshocks, Aftershocks, and Source

811   Models. Seismological Research Letters 88 (3), 757–771 (2017).

812

813   Chiodini, G., Cioni, R., Guidi, M., Raco, B., Marini, L., Soil CO_2 flux measurements in volcanic and

814   geothermal areas. Appl. Geochem. 13, 543-552 (1998).

815

816   Chiodini, G., Cardellini, C., Di Luccio, F., Selva, J., Frondini, F., Caliro, S., Rosiello, A., Beddini, G.,

817   Ventura, G., Correlation between tectonic CO_2 Earth degassing and seismicity is revealed by a 10-

818   year record in the Apennines, Italy. Sci. Adv. 6:eabc2938, 1-7, doi:10.1126/sciadv.abc2938 (2020).

819

820   Comerci, V., Doglioni, C., Italiano, F., Baiocco, F., Barberio, M.D., Caracausi, A., Cuiuli, E., Guerra,

821   M., Infantino, V., Insolvibile, M., Marcaccio, M., Martinelli, G., Menichetti, S., Onorati, G., Petitta,

822   M., Palumbo, V., Peleggi, M., Richieri, F., Scaramella, A., Scotti, E., Testa, M., Towards a national

823   hydrogeochemical monitoring system: a further tool to investigate geological hazards. Misc. INGV

824   49, 1-338 (2019).

825

826   D'Alessandro, A., Scudero, S., Siino, M., Alessandro, G., Mineo, R., Long-term monitoring and

827   characterization of soil radon emission in a seismically active area. Geochem. Geophy. Geosy.

828   21:e2020GC009061, doi:10.1029/2020GC009061 (2020).

829

830   D'Agostino, N., Avallone, A., Cheloni, D., D'Anastasio, E., S Mantenuto, Selvaggi, G., Active

831   tectonics of the Adriatic region from GPS and earthquake slip vectors. Jour. Geophys. Res. 113 (B12),

832   B12413 (2008).

833

834   Danecek, P., Pintore, S., Mazza, S., Mandiello, A., Fares, M., Carluccio, I., ... & Michelini, A., The

835   Italian node of the European integrated data archive. Seismological Society of America, 92(3), 1726-

836   1737, doi:https://doi.org/10.1785/0220200409 (2021).

837

838   Danesi, S., Pondrelli, S., Salimbeni, S., Cavaliere, A., Serpelloni, E., Danacek P., Lovati, S., Massa,

839   M., Active deformation and seismicity in the Southern Alps (Italy): The Montello hill as a case study.

840   Tectonophysics 653, 95-108, doi:10.1016/j.tecto.2015.03.028 (2015).

841

842   De Gregorio, S., Gurrieri, S., Valenza, M., A PTFE membrane for the in situ extraction of dissolved

843   gases in natural waters: Theory and applications. Geochem. Geophys. Geosyst., 6, Q09005,

844   doi:10.1029/2005GC000947 (2005).

845

846   De Gregorio, S., Federico, C., Cappuzzo, S., Favara, R., Giudice, G., Gurrieri, S., Boschi, E., Stress-

847   induced temperature variations in groundwater of the Monferrato area (north-western Italy).

848   Geofluids 12, 142-149, doi:10.1111/j.1468-8123.2011.00348.x (2012).

849

850   De Luca, G., Di Carlo, G., Tallini, M., A record of changes in the Gran Sasso groundwater before,

851   during and after the 2016 Amatrice earthquake, central Italy. Sci. Rep. UK 8:15982, 1-16,

852   doi:10.1038/s41598-018-34444-1 (2018).

853

854   De Matteis, R., Convertito, V., Napolitano, F., Amoroso, O., Terakawa, T., Capuano, P., Pore fluid

855   pressure imaging of the Mt. Pollino region (southern Italy) from earthquake focal mechanisms.

856   Geophys. Res. Lett. 48:e 2021GL094552, doi:10.1029/2021GL094552 (2021).

857

858   Di Luccio, F., Ventura, G., Di Giovambattista, R., Piscini, A., Cinti, F.R., Normal faults and thrusts

859   reactivated by deep fluids: The 6 April 2009 M_w 6.3 L'Aquila earthquake, central Italy. J. Geophys.

860   Res. 115, 1-15, doi:10.1029/2009JB007190 (2010).

861

862   DISS Working Group Database of Individual Seismogenic Sources (DISS), Version 3.3.0: A

863   compilation of potential sources for earthquakes larger than M 5.5 in Italy and surrounding areas.

864   Istituto Nazionale di Geofisica e Vulcanologia (INGV) https://doi.org/10.13127/diss3.3.0 (2021).

865

866   Egidio, E., Mancini, S., De Luca, D.A., Lasagna, M., The Impact of Climate Change on Groundwater

867   Temperature of the Piedmont Po Plain (NW Italy). Water 14:2797, doi:10.3390/w14182797 (2022).

868

869   Ferrari E., Massa M., Rizzo A.L., Lovati S., Di Michele F. The Italian multiparametric network for

870   detection and monitoring of earthquake-related crustal fluids alterations. EGU meeting, Wien, session

871   SM3.4, 14-19 April (2024).

872

873   Gabrielli, S., Akinci, A., Ventura, G., Napolitano, F., Del Pezzo, E., De Siena, L., Fast changes in

874   seismic attenuation of the upper crust due to fracturing and fluid migration: the 2016–2017 Central

875   Italy seismic sequence. Front. Earth Sci. 10:909698, doi: 10.3389/feart.2022.909698 (2022).

876

877   Gabrielli, S., Akinci, A., De Siena, L., Del Pezzo, E., Buttinelli, M., Maesano, F.E., Maffucci, R.,

878   Scattering attenuation images of the control of thrusts and fluid overpressure on the 2016–2017

879   Central   Italy   seismic   sequence.   Geophys.   Res.   Lett.   50:e2023GL103132,

880   doi:10.1029/2023GL103132 (2023).

881

882   Galadini, F., Galli, P., The Holocene paleoearthquakes on the 1915 Avezzano earthquake faults

883   (central Italy): implications for active tectonics in the central Apennines. Tectonophysics 308, 1-2,

884   143-170 (1999).

885

886   Galadini, F., Messina, P., Plio-Quaternary changes of the normal fault architecture in the Central

887   Apennines (Italy). Geodinamica Acta, 321-344, https://doi.org/10.1080/09853111.2001.10510727

888   (2001).

889

890   Galli, P., Galderisi, A., Ilardo, I., Piscitelli, S., Scionti, V., Bellanova, J., & Calzoni, F., Holocene

891   paleoseismology of the Norcia fault system (central Italy). Tectonophysics 745, 154-169,

892   https://doi.org/10.1016/j.tecto.2018.08.008 (2018).

893

894   Galli, P., Galderisi, A., Peronace, E., Giaccio, B., Hajdas, I., Messina, P., Pileggi, D., Polpetta, F. The

895   Awakening of the Dormant Mount Vettore Fault (2016 Central Italy Earthquake, Mw 6.6):

896   Paleoseismic Clues on Its Millennial Silences. Tectonics https://doi.org/10.1029/2018TC005326

897   (2019).

898

899   Gerten, D., Hoff, H., Rockström, J., Jägermeyr, J., Kummu, M., Pastor, A.V., Towards a revised

900   planetary boundary for consumptive freshwater use: role of environmental flow requirements.

901   Environmental Sustainability 5, issue 6, 551-558 (2013).

902

903   Giambastiani, B.M.S., Chiapponi, E., Polo, F., Nespoli, M., Piombo, A., Antonellini, M., Structural

904   control on carbon emissions at the Nirano mud volcanoes – Italy. Marine and Petroleum Geology

905   163, 106771 (2024).

906

907   Goldstein, P., Dodge, D., Firpo, M., Minner, L., SAC2000: Signal processing and analysis tools for

908   seismologists and engineers, Invited contribution to "The IASPEI International Handbook of

909   Earthquake and Engineering Seismology", Edited by WHK Lee, H. Kanamori, P.C. Jennings, and C.

910   Kisslinger, Academic Press, London (2003).

911

912   Gori, F., Barberio, M.D., Hydrogeochemical changes before and during the 2019 Benevento seismic

913   swarm in central-southern Italy. J. Hydrol. 604:127250, 1-10, doi:10.1016/j.jhydrol.2021.127250

914   (2022).

915

916   Guillaumot, L., Longuevergne, L., Marçais, J., Lavenant, N., Bour, O., Frequency domain water table

917   fluctuations reveal impacts of intense rainfall and vadose zone thickness on groundwater recharge.

918   Hydrology and Earth System Sciences 26, issue 22, HESS, 26, 5697–5720,

919   https://doi.org/10.5194/hess-26-5697-2022 (2022).

920

921   Hubbert, M.K., Rubey, W.W., Role of fluid pressure in mechanics of overthrust faulting: mechanics

922   of fluid-filled porous solids and its application to overthrust faulting. Geol. Soc. Am. Bull. 70(2), 115-

923   166, doi:10.1130/0016-7606(1959)70[115:ROFPIM] 2.0.CO;2 (1959).

924

925   Improta, L. and co-Authors Multi-segment rupture of the 2016 Amatrice-Visso-Norcia seismic

926   sequence (central Italy) constrained by the first high-quality catalog of Early Aftershocks. Scientific

927   Reports, 9, 6921 (2019).

928

929   Inguaggiato, S., Vita, F., Rouwet, D., Bobrowski, N., Morici, S., Sollami, A., Geochemical evidence

930   of the renewal of volcanic activity inferred from CO2 soil and SO2 plume fluxes: the 2007 Stromboli

931   eruption (Italy). Bulletin of Volcanology http://dx.doi.org/10.1007/s00445-010-0442-z (2011a).

932

933   Inguaggiato, S., Calderone, L., Inguaggiato, C., Morici, S. and Vita, F., Dissolved CO_2 in natural

934   waters: development of an automated monitoring system and first application to Stromboli volcano

935   (Italy). Annals of Geophysics 54(2), doi: 10.4401/ag-5180 (2011b).

936

937   Italiano, F., Martinelli, G., Rizzo, A., Geochemical evidence of seismogenic-induced anomalies in the

938   dissolved gases of thermal waters: A case study of Umbria (Central Apennines, Italy) both during and

939   after the 1997-1998 seismic swarm. Geochem. Geophy. Geosy. 5(11), 1-11,

940   doi:10.1029/2004GC000720 (2004).

941

942   Italiano, F., Martinelli, G., Nuccio, P.M., Anomalies of mantle-derived helium during the 1997-1998

943   seismic swarm of Umbria-Marche, Italy. Geophy. Res. Lett. 28(5), 839-842,

944   doi:10.1029/2000GL012059 (2001).

945

946   Keranen, K.M., Weingarten, M., Induced seismicity. Annu. Rev. Earth Pl. Sc. 46, 149-174.

947   doi:10.1146/annurev-earth-082517-010054 (2018).

948

949   King, C.Y., Gas geochemistry applied to earthquake prediction: An overview, Journal of Geophysical

950   Research. https://doi.org/10.1029/JB091iB12p12269 (1986).

951

952   Lai, C.G., Poggi, V., Famà, A., Zuccolo, E., Bozzoni, F., Meisina, C., Bonì, R., Martelli, L., Massa,

953   M., Mascandola, C., Petronio, L., Affatato, A., Baradello, L., Castaldini, D., Cosentini, R.M., An

954   inter-disciplinary and multi-scale approach to assess the spatial variability of ground motion for

955   seismic microzonation: the case study of Cavezzo municipality in Northern Italy, Eng. Geol. 274,

956   105722, https://doi.org/10.1016/j.enggeo.2020.105722 (2020).

957

958   Lee, H.A., Hamm, S.Y., Woo, N.C., Pilot-scale groundwater monitoring network for earthquake

959   surveillance and forecasting research in Korea. Water 13:2448, 1-19, doi:10.3390/w13172448

960   (2021).

961

962   Locati, M., Camassi, R., Rovida, A., Ercolani, E., Bernardini, F., Castelli, V., Caracciolo, C.H.,

963   Tertulliani, A., Rossi, A., Azzaro, R., D'Amico, S., Conte, S., Rocchetti, E., Antonucci, A., Database

964   Macrosismico Italiano (DBMI15), versione 4.0. Istituto Nazionale di Geofisica e Vulcanologia

965   (INGV), https://doi.org/10.13127/dbmi/dbmi15.4 (2022).

966

967   Luzi, L., Pacor, F., Ameri, G., Puglia, R., Burrato, P., Massa, M., Augliera, P., Castro, R.,

968   Franceschina, G., Lovati, S. Overview on the strong motion data recorded during the May-June 2012

969   Emilia seismic sequence. Seism. Res. Lett., 84, 4, 629-644 (2013).

970

971   Luzi, L., Puglia, R., Russo, E., D'Amico, M., Felicetta, C., Pacor, F., Lanzano, G., Çeken, U.,

972   Clinton, J., Costa, G., et al. The European strong-motion database: a platform to access accelerometric

973   data. Seismol. Res. Lett. 87, 4, doi: 10.1785/0220150278 (2016).

974

975   Malagnini, L., Pio Lucente, F., De Gori, P., Akinci, A., Munafo', I., Control of pore fluid pressure

976   diffusion on fault failure mode: Insights from the 2009 L'Aquila seismic sequence. J. Geophys. Res-

977   Sol. Ea. 117, 1-15, doi:10.1029/2011JB008911 (2012).

978

979   Mancini, S., Egidio, E., De Luca, D.A., Lasagna, M., Application and comparison of different

980   statistical methods for the analysis of groundwater levels over time: Response to rainfall and resource

981   evolution in the Piedmont Plain (NW Italy). Science of the total Environment 846, 157479 (2022).

982

983   Marchetti, A. and co-Authors The Italian Seismic Bulletin: strategies, revised pickings and locations

984   of the central Italy seismic sequence. Annals of Geophysics FAST TRACK 5/59, 10.4401/ag-7169

985   (2016).

986

987   Margheriti, L. and co-Authors Seismic Surveillance and Earthquake Monitoring in Italy.

988   Seismological Research Letters 92 (3): 1659-1671 (2021).

989

990   Martinelli, G., Contributions to a history of earthquake prediction research. In Pre-earthquake

991   processes: a multidisciplinary approach to earthquake prediction studies. Editors Ouzounov, D.,

992   Pulinets, S., Hattori, K., Taylor, P. John Wiley & Sons (2018).

993

994   Martinelli, G., Ciolini, R., Facca, G., Fazio, F., Gherardi, F., Heinicke, J., Pierotti, L., Tectonic-related

995   geochemical and hydrological anomalies in Italy during the last fifty years. Minerals 11:107, 1-16,

996   doi:10.3390/min11020107 (2021).

997

998   Massa M., Rizzo L.A., Ferrari E., Lovati S., Scafidi D., Puglia R., Varchetta F., D'Alema E., Mirenna

999   S., Luzi L., MUDA geophysical and geochemical MUltiparametric DAtabase,

1000   https://doi.org/10.13127/muda (2023).

1001

1002   Massa, M., Marzorati,S., D'Alema, E., Di Giacomo, D., Augliera, P., Site Classification Assessment

1003   for Estimating Empirical Attenuation Relationships for Central-Northern Italy Earthquakes. Journal

1004   Earth. Eng. 11:6, 943-967 (2007).

1005

1006 Massa, M., Rizzo, A.L., Lorenzetti, A., Lovati, S., D'Alema, E., Puglia, R., Carannante, S., Piersanti,

1007 A., Galli, G., Cannelli, V., Luzi, L., blog INGV Terrermoti, https://ingvterremoti.com/2021/12/10/la-

1008 rete-del-lago-di-garda-una-nuova-infrastruttura-dellingv-per-il-monitoraggio-multiparametrico/ (in

1009 Italian) (2021).

1010

1011 Massa, M., Lovati, S., Puglia, R., Brunelli, G., Lorenzetti, A., Mascandola, C., Felicetta, C., Pacor,

1012 F., Luzi, L., Seismo-Stratigraphic Model for the Urban Area of Milan (Italy) by Ambient-Vibration

1013 Monitoring and Implications for Seismic Site Effects Assessment. Frontiers in Earth Science doi:

1014 10.3389/feart.2022.915083 (2022b).

1015

1016 Massa, M., Scafidi, D., Mascandola, C., Lorenzetti, A., Introducing ISMDq—A Web Portal for Real-

1017 Time Quality Monitoring of Italian Strong-Motion Data. Seismol. Res. Lett. 93 (1), 241-256,

1018 doi:10.1785/0220210178 (2022).

1019

1020 Mastrorillo, L., Saroli, M., Viaroli, F., Banzato, F., Valigi, D., Petitta, M., Sustained post-seismic

1021 effects on groundwater flow in fractured carbonate aquifers in Central Italy. Hydrological Processes

1022 https://doi.org/10.1002/hyp.13662 (2020).

1023

1024 Mazzoli, S., Santini, S., Macchiavelli, C., Ascione, A., Active tectonics of the outer northern

1025 Apennines: Adriatic vs. Po Plain seismicity and stress fields. Journal of Geodynamics 84, 62-76

1026 (2015).

1027

1028 McNamara, D.E., Buland, R.P., Ambient Noise Levels in the Continental United States. Bull. Seism.

1029 Soc. Am. 94, 4, 1517-1527, https://doi.org/10.1785/012003001 (2004).

1030

1031   Menberg, K., Blum, P., Kurylyk, B.L., Bayer, P., Observed groundwater temperature response to

1032   recent climate change. Hydrol. Earth Syst. Sci. 18, 4453-4466, doi:10.5194/hess-18-4453-2014

1033   (2014).

1034

1035   Michelini, A., Faenza, L., Lanzano, G., Lauciani, V., Jozinović D., Puglia, R., Luzi, L., The New

1036   ShakeMap in Italy: Progress and Advances in the Last 10 Yr. Seismological Research Letters 91 (1),

1037   317-333 (2020).

1038

1039   Miller, S.A., Collettini, C., Chiaraluce, L., Cocco, M., Barchi, M., Kaus, B.J.P., Aftershocks driven

1040   by a high-pressure CO_2 source at depth. Nature 427, 724-727, doi:10.1038/nature02251 (2004).

1041

1042   Ministero delle Infrastrutture e dei Trasporti Aggiornamento delle Norme Tecniche per le

1043   Costruzioni. Part 3.2.2: Categorie di sottosuolo e condizioni topografiche (in Italian), Gazzetta

1044   Ufficiale n. 42 (2018).

1045

1046   Massa M., Rizzo L.A., Ferrari E., Lovati S., Scafidi D., Puglia R., Varchetta F., D'Alema E., Mirenna

1047   S., Luzi L, MUDA: geophysical and geochemical MUltiparametric Database,

1048   https://doi.org/10.13127/muda (2023).

1049

1050   Napolitano, F., De Siena, L., Gervasi, A., Guerra, I., Scarpa, R., La Rocca, M., Scattering and

1051   absorption imaging of a highly fractured fluid-filled seismogenetic volume in a region of slow

1052   deformation. Geosci. Front. 11, 989-998, doi:10.1016/j.gsf.2019.09.014 (2020).

1053

1054   Pacor, F., Paolucci, R., Ameri, G., Massa, M., Puglia R., Italian strong motion records in ITACA:

1055   Overview and record processing. Bull. Earthq. Eng. 9, 6, 1741-1759 (2011).

1056

1057   Pessina, V., Fiorini, E., A GIS procedure for fast topographic characterization of seismic recording

1058   stations. Soil Dynam. Earthq. Eng. 63, 248-258 (2014).

1059

1060   Pieri, M., Groppi, G., Subsurface Geological Structure of the Po Plain, Italy. Progetto Finalizzato

1061   Geodinamica/Sottoprogetto "Modello Strutturale" (Rome: Consiglio Nazionale delle Ricerche Publ.

1062   N° 414) (1981).

1063

1064   Pondrelli, S., Ekström, G., Morelli, A., Seismotectonic re-evaluation of the 1976 Friuli, Italy, seismic

1065   sequence. Journal of Seism., 5, 73-83 (1999).

1066

1067   Rikitake, T., Hamada, K., Earthquake prediction. In: Encyclopaedia of Physical Science and

1068   Technology, 3rd edition, Academic Press, San Diego, CA, USA 4, 743-760 (2001).

1069

1070   Rizzo, A.L., Federico, C., Inguaggiato, S., Sollami, A., Tantillo, M., Vita, F., Bellomo, S., Longo,

1071   M., Grassa, F., Liuzzo, M., The 2014 Effusive Eruption at Stromboli Volcano (Italy): Inferences From

1072   Soil CO_2 Flux and 3He/4He Ratio in Thermal Waters. Geoph. Res. Lett.

1073   http://dx.doi.org/10.1002/2014GL062955 (2015).

1074

1075   Romano, D., Sabatino, G., Magazù, S., Di Bella, M., Tripodo, A., Gattuso, A., Italiano, F.,

1076   Environmenta Earth Sciences 82, 273 (2023).

1077

1078   Russo, T.A., Lall, U., Depletion and response of deep groundwater to climate-induced pumping

1079   variability. Nature Geoscience 10, 105-108 (2017).

1080

1081   Rovida, A., Locati, M., Camassi, R., Lolli, B., Gasperini, P., The Italian Earthquake Catalogue

1082   CPTI15. Bull. Earthq. Eng. 18 (7), 2953-2984, doi:10. 1007/s10518-020-00818-y (2020).

1083

1084   Scognamiglio, L., Tinti, E., Michelini, A., Dreger, D.S., Cirella, A., Cocco, M., Salvatore, M.,

1085   Piatanesi, A., Fast Determination of Moment Tensors and Rupture History: What Has Been Learned

1086   from the 6 April 2009 L'Aquila Earthquake Sequence. Seism. Res. Lett. 81(6): 892-906 (2009).

1087

1088   Serpelloni, E., Anzidei, M., Baldi, P., Casula, G., Galvani, A., Crustal Velocity and Strain-Rate fields

1089   in Italy and Surrounding Regions: New Results From the Analysis of Permanent and Non- Permanent

1090   GPS Networks. Geophys. J. Int., 161, 3, 861-880 (2005).

1091

1092   Shinohara, H., A new technique to estimate volcanic gas composition: plume measurements with a

1093   portable multi-sensor system. J. Volcanol. Geotherm. Res. 143, 319-333 (2005).

1094

1095   Skelton, A., and co-Authors Changes in groundwater chemistry before two consecutive earthquakes

1096   in Iceland. Nature Geoscience 7, 752-756 (2014).

1097

1098   Stucchi, M., Meletti, C., Montaldo, V., Crowley, H., Calvi, G.M., Boschi, E., Seismic Hazard

1099   Assessment (2003-2009) for the Italian building code. Bull. Seism. Soc. Am. 101, 1885-1911 (2011).

1100

1101   Taylor, C.A., Stefan, H.G., Shallow groundwater temperature response to climate change and

1102   urbanization. J. Hydrol. 375, 601-612, doi:10.1016/j.jhydrol.2009.07.009 (2009).

1103

1104   Ventura, G., Di Giovambattista, R., Fluid pressure, stress field and propagation style of coalescing

1105   thrusts from the analysis of the 20 May 2012 M_L 5.9 Emilia earthquake (Northern Apennines, Italy).

1106   Terra Nova 25, 72-78, doi: 10.1111/ter.12007 (2012).

1107

1108   Weiss, A., Topographic position and landform analysis. 21st Annual Esri International User

1109   Conference, San Diego, California, 9-13 July (2001).

1110

1111   **Figure Captions**

1112

1113   **Figure 1 -** MUDA home page: https://muda.mi.ingv.it. Examples of interactive pop-ups are reported

1114   in map indicating the available main options concerning stations data and metadata, Italian seismic

1115   hazard (Stucchi et al., 2011), seismicity rate and both composite and single seismogenic sources

1116   (DISS database, DISS Working Group 2021). The base map is provided by ©OpenStreetMap

1117   contributors 2024. Distributed under the Open Data Commons Open Database License (ODbL) v1.0.

1118

1119   **Figure 2** - Target areas and relative multiparametric sites. Each panel indicates the multiparametric

1120   site (yellow triangles), the Italian seismic hazard map in terms of horizontal peak ground acceleration

1121   (PGA) with 10% probability of exceedance in 50 years on hard ground (Stucchi et al., 2011), the

1122   instrumental seismicity from 1985 (black circles, https://terremoti.ingv.it), the historical seismicity

1123   (red circles, CPTI database, Rovida et al., 2020) and the seismogenic sources (CSS-DISS database,

1124   DISS Working Group 2021). The base maps are provided by ©OpenStreetMap contributors 2024.

1125   Distributed under the Open Data Commons Open Database License (ODbL) v1.0.

1126

1127   **Figure 3** - Dynamic multiparametric data web page: https://muda.mi.ingv.it/dat.php. From top to

1128   bottom: hydrogeochemical data (light blue panels: water level, m; water electrical conductivity,

1129   µS/cm; water temperature, °C), meteorological data (green panel: soil temperature, °C; rain, mm),

1130   seismic data (light brown panels: RMS, ground motion velocity, cm/s; FFT, cm/s/Hz; FFT(f),

1131   cm/s/Hz), CO_2 data (grey panels: soil flux, $g*m^{-2}*d^{-1}$; humidity, %; soil temperature, °C), Radon data

1132   on air (yellow panel: Bq/m^3). All time series (*csv* format) and each single graph (*pdf*, *png* formats)

1133   are downloadable by using the menu available in the top right corner of each panel.

1134

1135   **Figure 4** - Multiparametric sites web page: https://muda.mi.ingv.it/stazione.php. The single site web

1136   page indicates the main features of both instrumentation and installation, downloadable thematic

1137   maps   such   as   the   geological   map   (1:100.000,   Società   Geologica   Italiana

1138   http://www.isprambiente.gov.it/it/cartografia/), the topographic map (base at 1:25.000, Istituto

1139   Geografico   Militare,   http://www.igmi.org/prodotti/cartografia/carte_topografiche/),   log   and

1140   stratigraphy concerning the available wells for water, a preliminary geophysical soil characterization

1141   in term of horizontal to vertical spectral ratio performed on ambient seismic noise and the complete

1142   time hydrogeochemical time series. Sources for base maps: Esri, DigitalGlobe, GeoEye, i-cubed,

1143   USDA FSA, USGS, AEX, Getmapping, Aerogrid, IGN, IGP, swisstopo, and the GIS User

1144   Community.

1145

1146   **Figure 5 -** MUDA data base scheme and processing flow chart.

1147

1148   **Figure 6** - Single station data set for multiparametric sites having at least 6 months of data and three

1149   different type of acquisition. S: seismic data (red); Id: hydrogeochemical data (blue); M:

1150   meteorological data (green); R: Radon data (grey); C: CO_2 data (yellow). Yellow and orange starts

1151   indicate recorded earthquakes at each site with magnitude (Moment or Local) lower and higher then

1152   4, respectively.

1153

1154   **Figure 7** - Quality check of seismic data at Oppeano site (table 1).

1155   Panel   *a*   (top):   timeseries   recorded   on   December,   29,   2020,   by   IV.OPPE   station

1156   (https://terremoti.ingv.it/instruments/station/OPPE) showing consecutive earthquakes: the first, with

1157 M_w=6.3, occurred in Croatia land (https://terremoti.ingv.it/event/25870121) 450 km East of IV.OPPE

1158   and   the   others   with   epicentres   11   km   South-West   of   IV.OPPE   with   maximum M_w=3.9

1159   (https://terremoti.ingv.it/event/25871441). Earthquakes origin times (UTC) are reported in the top

1160   panel *a*).

1161   The bottom panel *a*) shows the FFT functions calculated considering 15 frequency intervals from 0.1

1162   to 20 Hz, considering 288 consecutive 5 minutes-time windows (i.e. 24 hours) selected on the vertical

1163   component of motion.

1164   Panel *b*: from top to bottom, the RMS, the ground motion velocity and the mean FFT calculated for

1165   288 consecutive time windows with duration of 5 minutes. Red, blue and green indicate the vertical,

1166   the North-South and the East-West horizontal components of motion. The black solid lines indicate

1167   the cumulative functions.

1168

1169   **Figure 8** - Example of multiparametric data recorded at Bondo site (table 1). Panel *a* shows the

1170   hydrogeochemical data recorded in the time period from October, 15 to November, 15, 2023: black,

1171   red and green solid lines indicate the water level (m), the electrical conductivity (μS/cm) and the

1172   water temperature (°C) variations, respectively.

1173   The panel *b* shows the seismic data recorded at ZO.PDN3 station (table 2) on October, 31 and

1174   November, 1, 2023, while the panel *c* shows the polarization analysis in terms of rotated horizontal

1175   to vertical spectral ratio.

1176

1177   **Figure 9 -** Radon time series (Bq/m^3, black lines) recorded at Bondo (panel *a*) and Montelungo (panel

1178   *b*) multiparametric sites. Soil temperature (°C, green lines) and rain (mm, light blue lines) are also

1179   indicated. At the top of each panel seasons are indicated (Aut=Autumn, Win=Winter, Spr=Spring,

1180   Sum=Summer).

1181

1182   **Figure 10** - Panel *a*: CO_2 flux (g*m^{-2}*d^{-1}, black line) recorded at NIRANO multiparametric site. Red

1183   and green solid lines indicate the smoothing function of CO_2 flux and the temperature (°C),

1184   respectively. The orange box indicates the time window represented in the bottom panel.

1185   Panel *b*: detailed monitoring for period October, 25, 2023 to November, 15, 2023, where a seismic

1186   sequence, with maximum local magnitude of 3.5 (vertical yellow dashed lines) occurred in

1187   correspondence of the Nirano's Mud-Volcanoes. Dotted and dashed orange lines indicate the mean

1188   values +/- 1-standard deviation of CO_2 flux recorded during the analysed time period. Rain values

1189   (mm, light blue) and soil temperature (°C) are also indicated. Black dots indicate the CO_2 measures

1190   ($g*m^{-2}*d^{-1}$).

1191

1192   **Figure 11** - Groundwater recharge at Volargne (panel *a*) and Fonte (panel *b*) sites (table 1) recorded

1193   on October, 30, 2023. In both panels, black, red and green solid lines indicate the water level (m), the

1194   electrical conductivity (µS/cm) and the water temperature (°C) variations, respectively, while the blue

1195   solid lines indicate the cumulative rain.

1196

1197   **Table captions**

1198

1199   **Table 1** - Monitoring multiparametric sites at present include in MUDA.
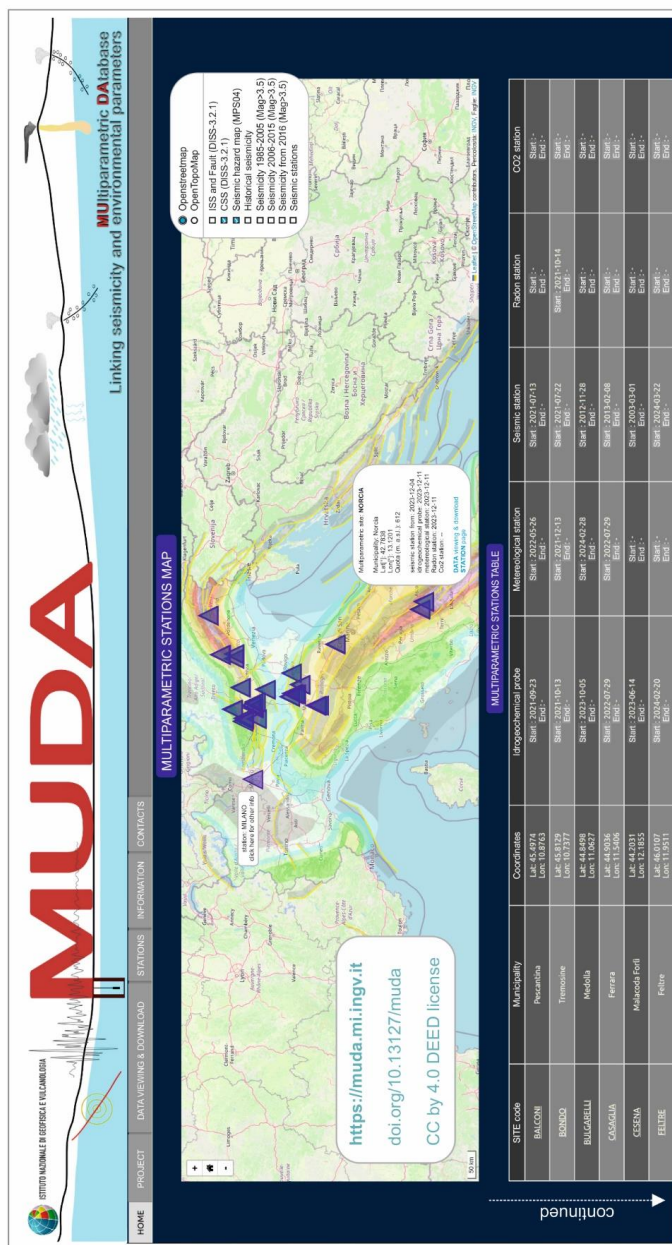
1200

1201   **Table 2** - Main features of hydrogeochemical probes and seismic monitoring stations. Grey cells

1202   indicate well with thermalism (i.e. Triponzo site), while the black cells indicate the borehole seismic

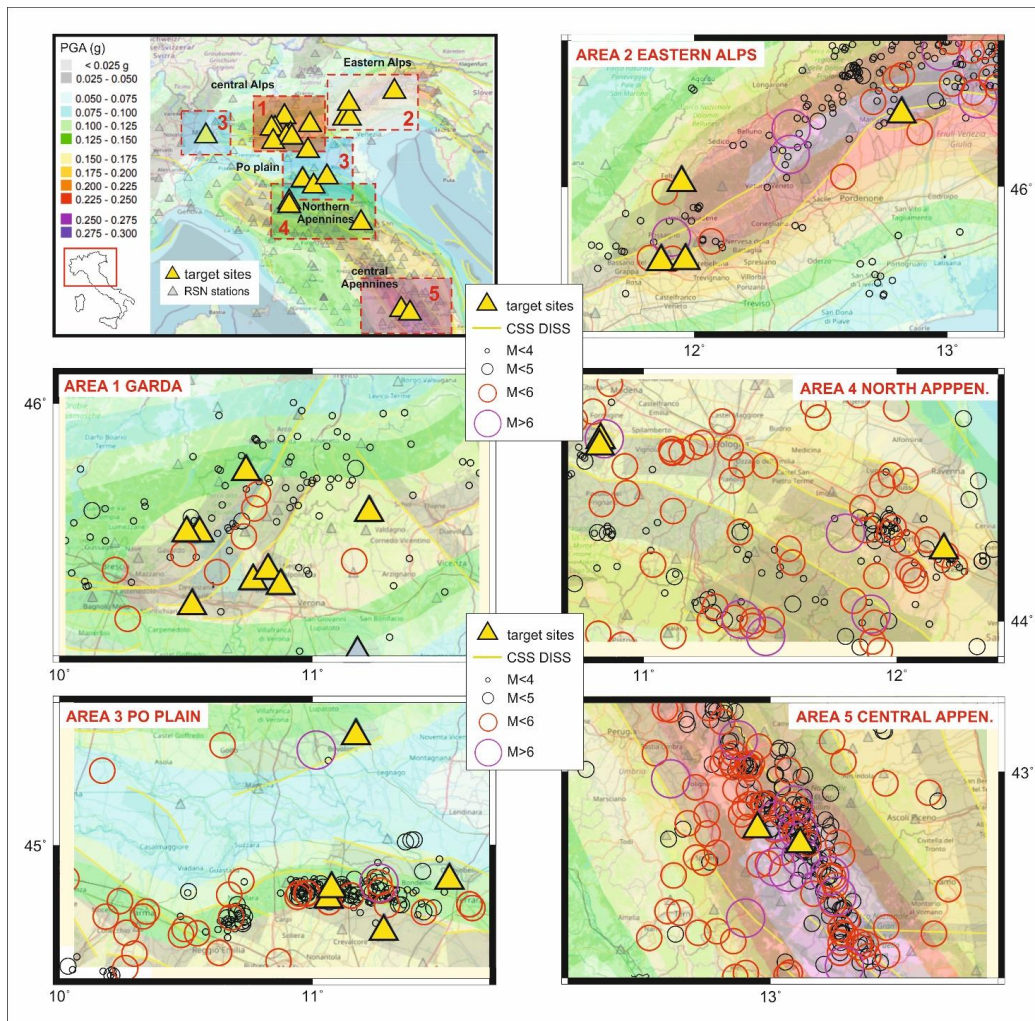1203   sensor installed 150 m depth at Oppeano site.

1204

1205

1206

1207

1208   Figure 1

1209

1210
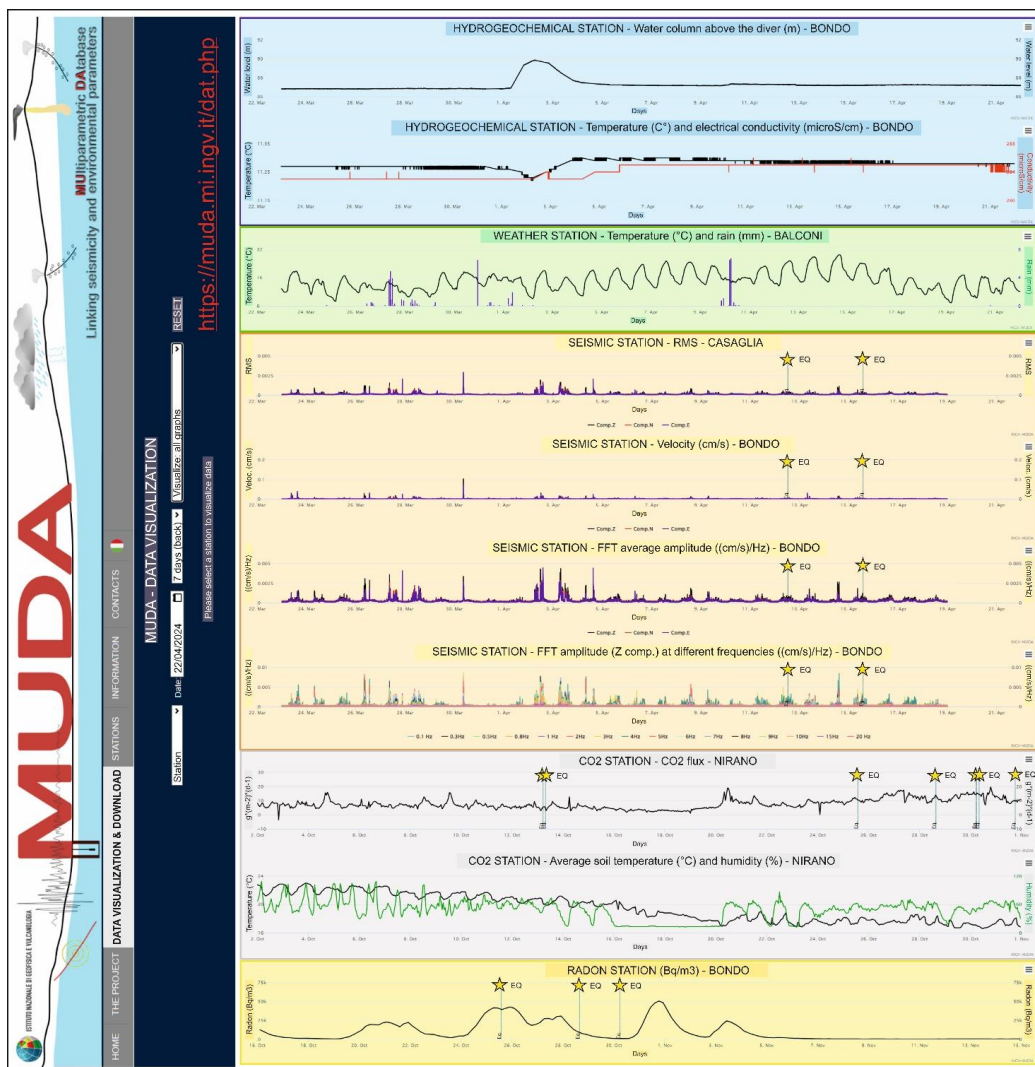
1211

1212   Figure 2

1213

1214

1215

1216

1217

1218

1219

1220

1221

1222   Figure 3

1223

1224

1225

1226

1227

1228

1229

1230

1231   Figure 4
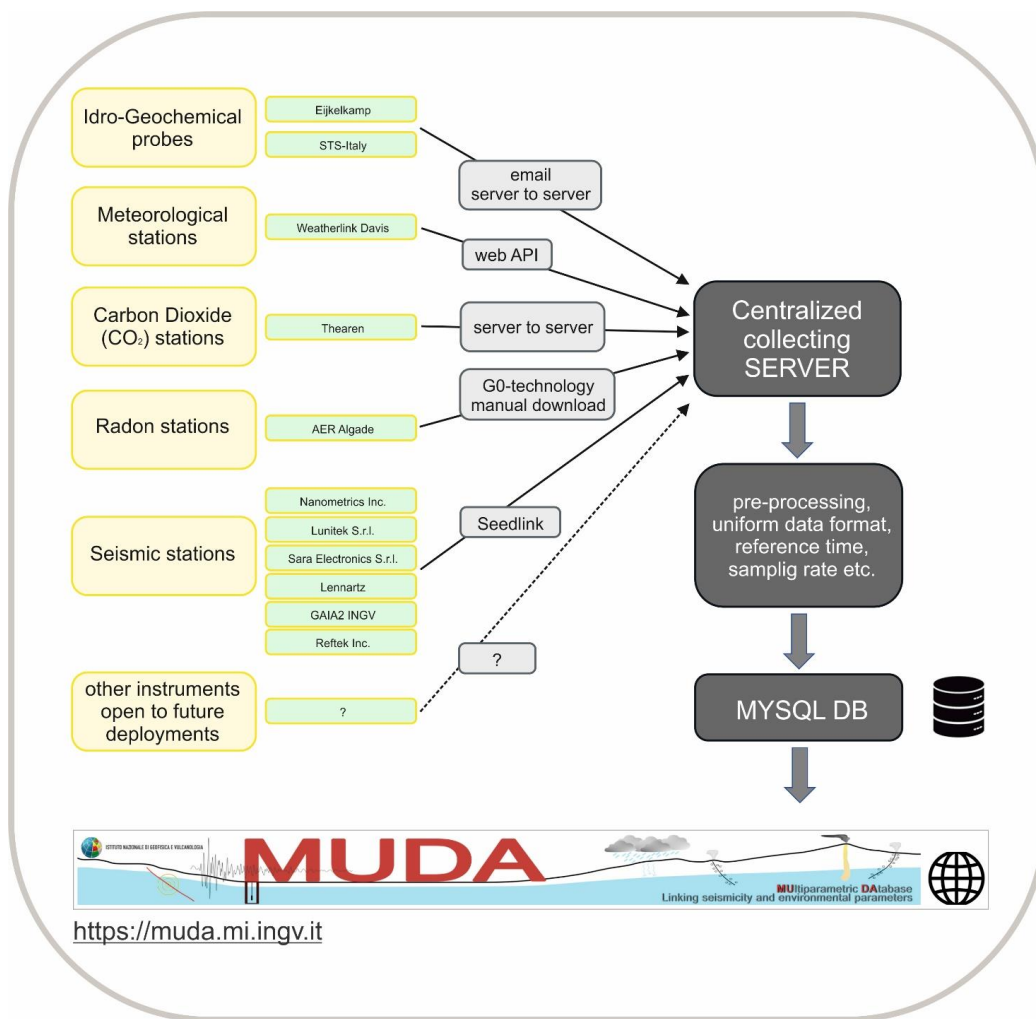
1232

1233

1234

1235

1236   Figure 5

1237

1238

1239

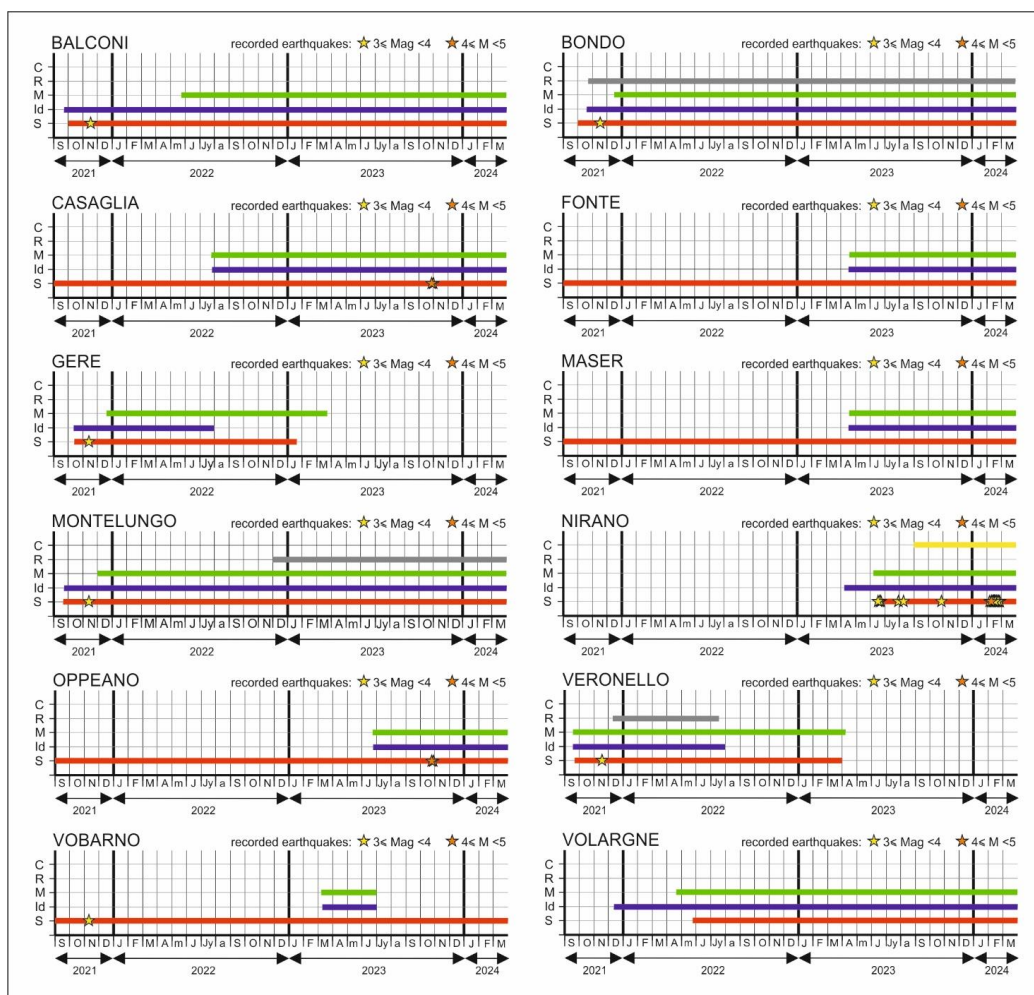1240

1241

1242

1243

1244

1245

1246   Figure 6

1247

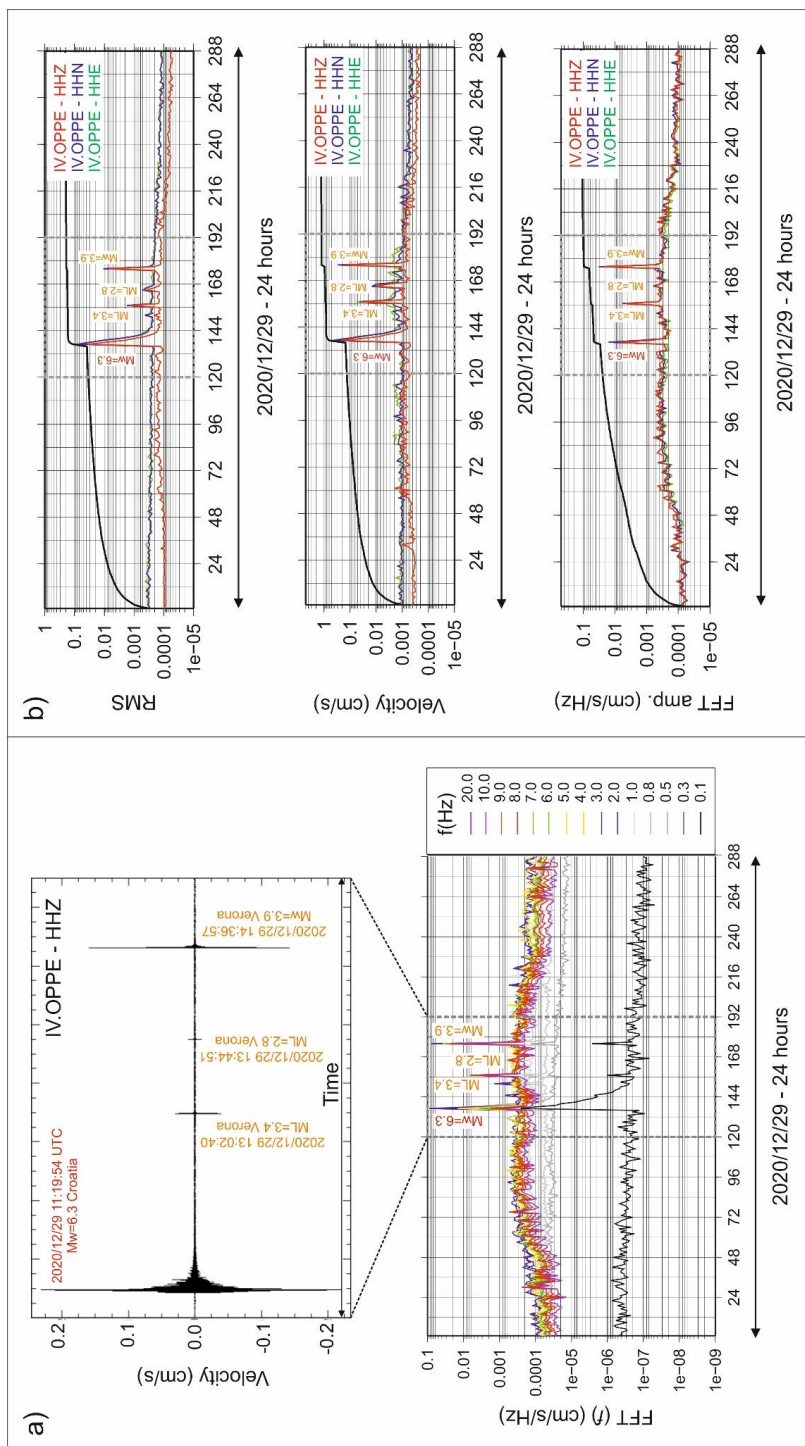1248

1249

1250

1251

1252

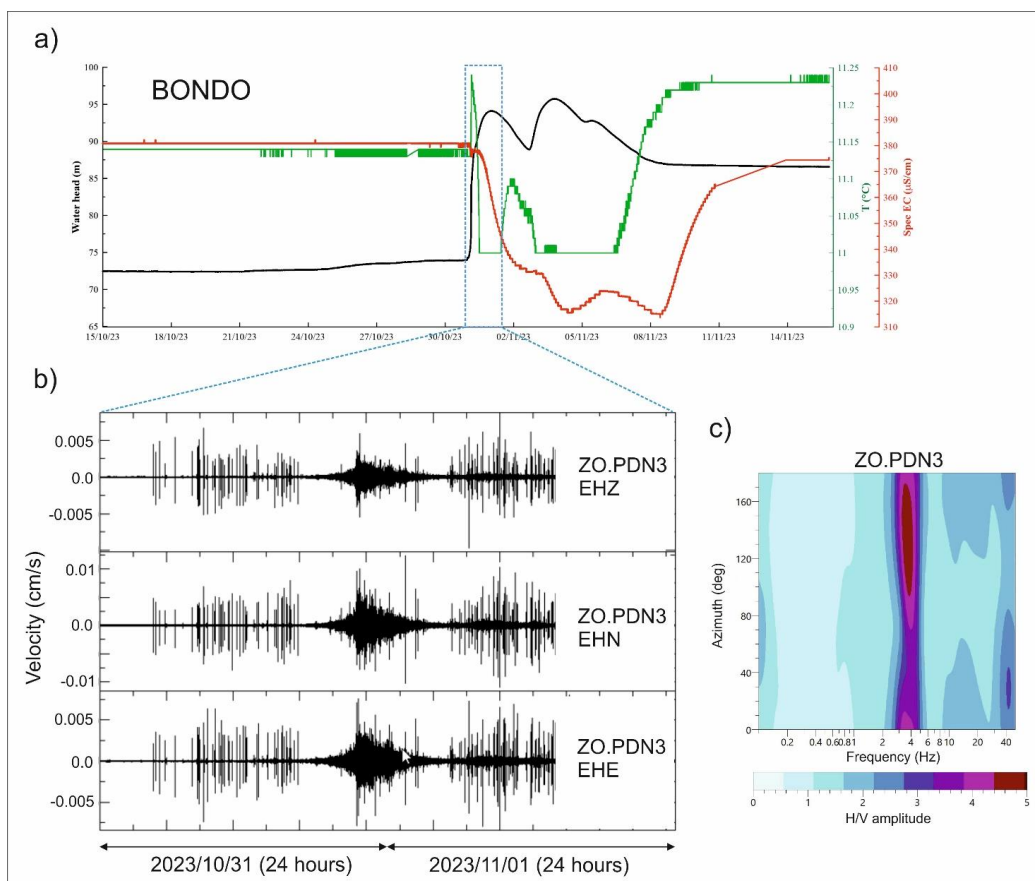1253

1254

1255

1256   Figure 7

54

1257

1258

1259   Figure 8

1260

1261

1262

1263
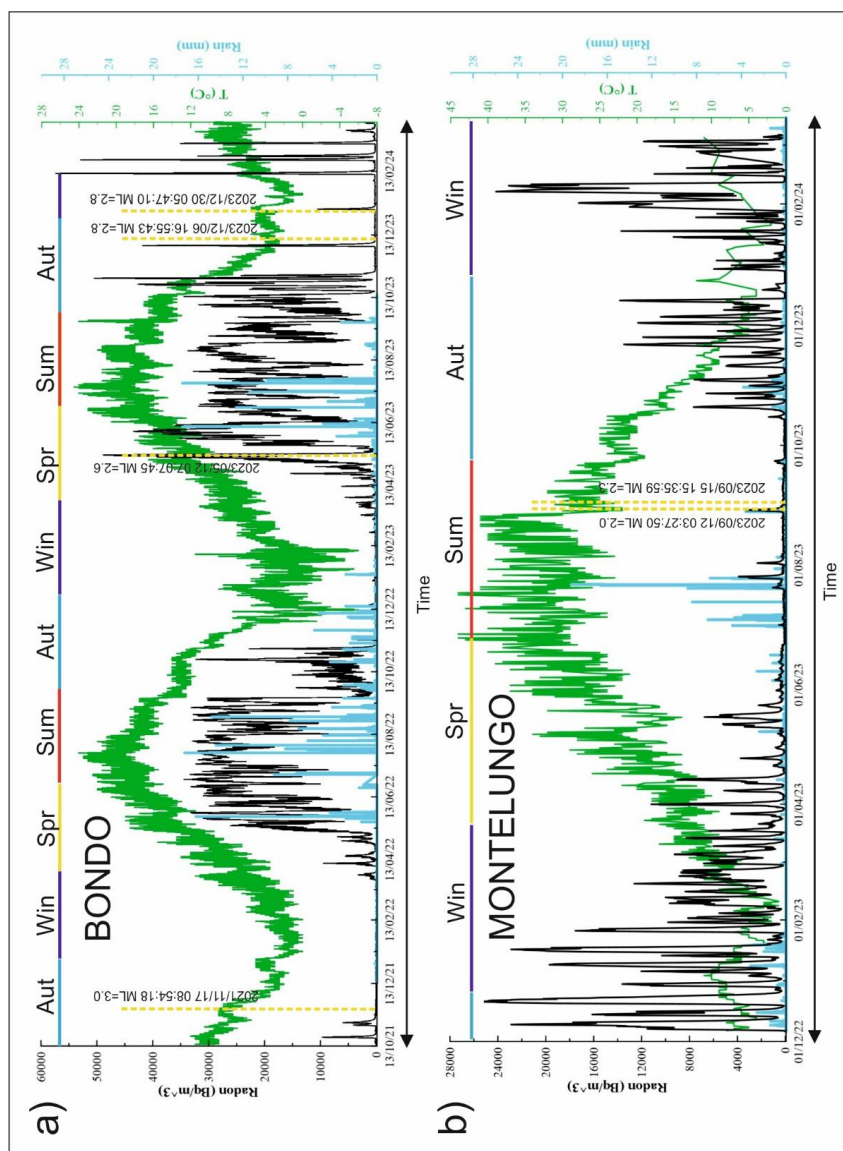
1264

1265

1266

1267

1268
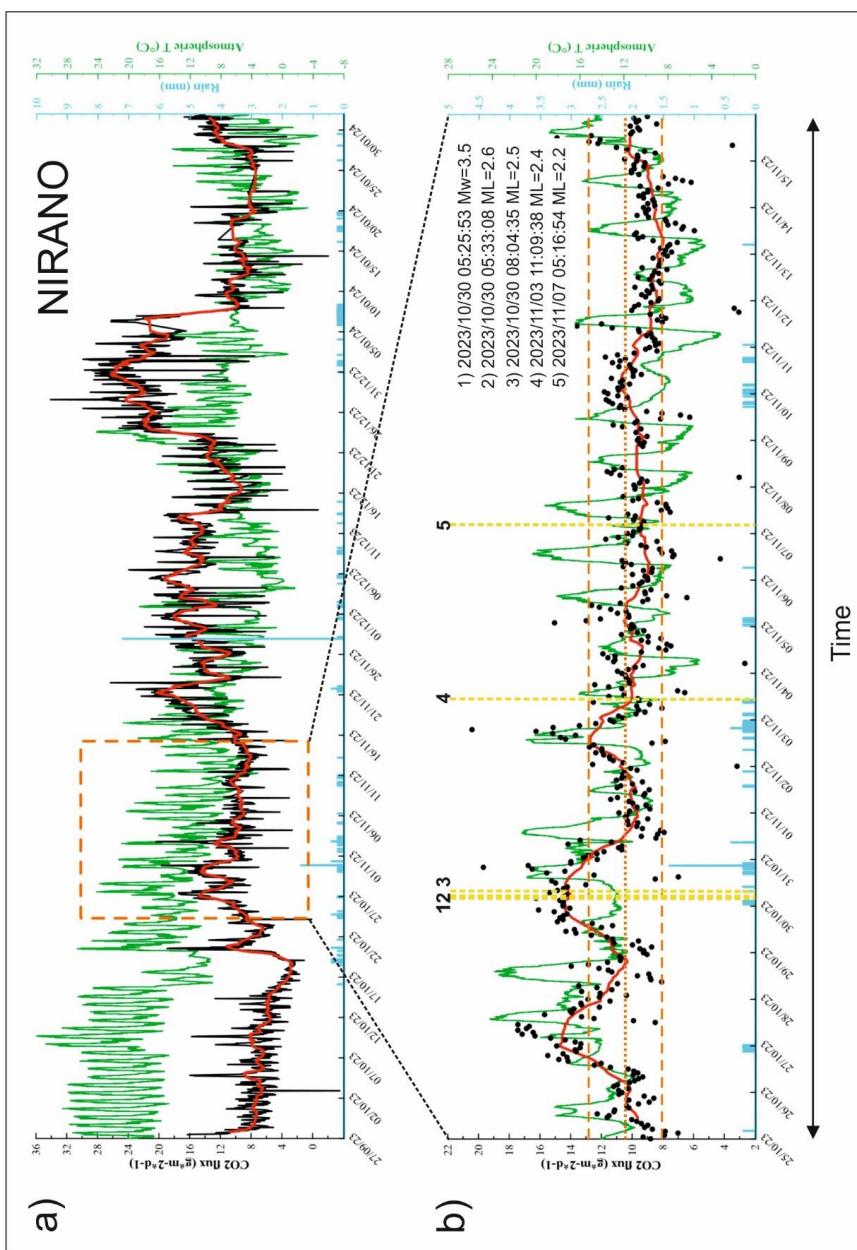
1269

1270

1271   Figure 9
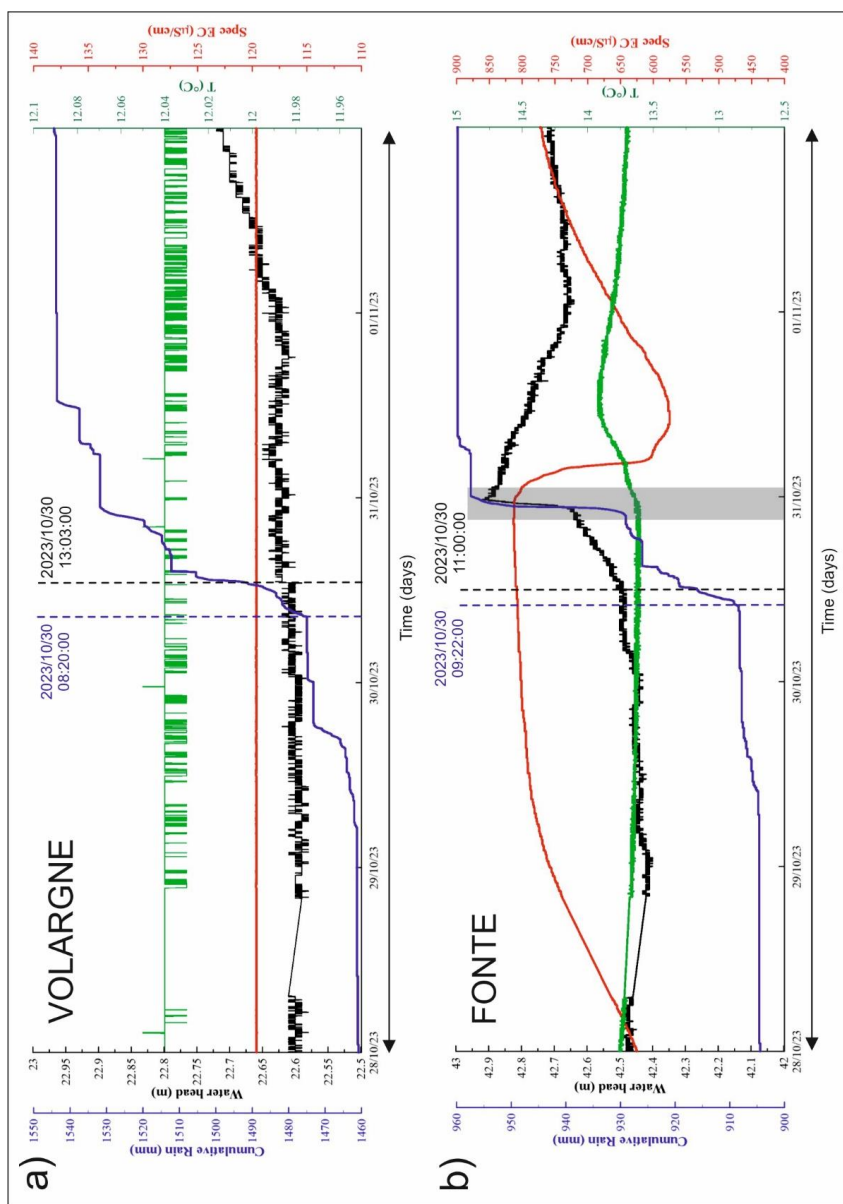
1272

1273

1274

1275

1276

1277

1278

1279   Figure 10

1280

1281

1282

1283

1284

1285   Figure 11

1286

1287

1288

Table 1

CODE	Municipality	AREA	LAT [°]	LON [°]	idro-geochemical	weather	seismic	Radon	CO2
BALCONI	Pescantina	1	45.4974	10.8763	start 2021-09-23	start 2022-05-26	start 2021-07-13	/	/
BONDO	Tremosine	1	45.8129	10.7377	start 2021-10-13	start 2021-12-13	start 2021-07-22	start 2021-10-14	/
BULGARELLI	Medolla	3	44.8498	11.0627	start 2024-02-28	start 2024-02-28	start 2012-11-28	/	/
CASAGLIA	Ferrara	3	44.9036	11.5406	start 2022-07-29	start 2022-07-29	start 2013-02-08	/	/
CESENA	Malacoda Forlì	4	44.2031	12.1855	start 2024-02-20	/	start 2003-03-01	/	/
FELTRE	Feltre	2	46.0107	11.9511	start 2024-02-20	/	/	/	/
FONTE	Fonte	2	45.7949	11.8697	start 2023-04-18	start 2023-04-17	start 2011-11-17	/	/
GERE	Gardone Riviera	1	45.6422	10.5484	start 2021-10-12 - end 2022-07-30	start 2021-12-02 - end 2023-03-25	start 2021-10-12 - 2023-01-18	/	/
MASER	Maser	2	45.7969	11.9658	start 2023-04-17	start 2023-04-17	start 2011-11-17	/	/
MEDOLLA	Medolla	3	44.8492	11.0734	start 2024-02-20	start 2024-02-28	start 2012-11-28	/	/
MILANO	Milano	3	45.4972	9.1812	start 2024-03-12	start 2024-03-12	start 2012-01-27	/	/
MIRANDOLA	Mirandola	3	44.8812	11.0782	start 2024-02-23	start 2024-02-23	start 2012-11-28	/	/
MONTELUNGO	Desenzano del Garda	1	45.4429	10.5256	start 2021-09-14	start 2021-11-30	start 2021-07-30	start 2022-12-06	/
NIRANO	Fiorano Modenese	4	44.5141	10.8255	start 2023-04-04	start 2023-06-06	start 2023-06-23	/	start 2023-09-27
NIRANO1	Fiorano Modenese	4	44.5002	10.8163	start 2024-02-20	start 2024-02-20	start 2023-06-23	/	/
NORCIA	Norcia	5	42.7838	13.1201	start 2023-12-11	start 2023-12-11	start 2023-12-04	start 2023-12-11	/
OPPEANO	Oppeano	3	45.3082	11.1723	start 2023-06-29	start 2023-06-21	start 2023-02-16	/	/
RECOARO	Recoaro Terme	1	45.6998	11.2217	start 2024-01-30	start 2024-01-30	/	/	/
RECOARO1	Recoaro Terme	1	45.7005	11.2215	start 2024-01-30	start 2024-01-30	/	/	/
RENAZZO	Renazzo	3	44.7624	11.2836	start 2024-02-20	/	start 2003-10-11	/	/
SECCHIA	Concordia Secchia	3	44.9245	11.0183	start 2024-03-14	start 2024-03-20	start 2012-11-28	/	/
TOPPO	Toppo di Travesio	2	46.1985	12.8171	start 2024-02-25	/	/	/	/
TRIPONZO	Triponzo	5	42.8400	12.9480	start 2023-12-12	start 2023-12-12	start 2023-12-04	start 2023-12-12	/
VERONELLO	Bardolino	1	45.5098	10.7645	start 2021-09-14 - end 2022-08-01	start 2021-10-19 - end 2023-04-07	start 2021-07-08 - end 2023-04-07	start 2021-12-17 - end 2022-07-08	/
VOBARNO	Vobarno	1	45.6428	10.5035	start 2023-03-10 - end 2023-06-21	start 2023-03-10 - end 2023-06-21	start 2021-07-08	/	/
VOLARGNE	Dolcè	1	45.5397	10.8235	start 2021-12-16	start 2022-05-20	start 2022-04-12	/	/

Table 2

CODE	AREA	Geology (100k)	Topography	SITE TYPE	WELL DEPTH (m)	WATER LEVEL (m)	WATER COLUM (m)	SEISMIC NET	SEISMIC CODE	RECORDER	SENSOR
BALCONI	1	fluvio-glacial deposits	plain	well	100	53.3	46.7	ZO	PDN2	Lunitek ATLAS	TELLUS-5s
BONDO	1	alluvial deposits	valley	well	180	44	136	ZO	PDN3	Reftek-130	LENNARTZ-5s
BULGARELLI	3	alluvial deposits	plain	well	8	1.5	6.5	IV	CAVE	GAIA2	TRILLIUM-120s
CASAGLIA	3	alluvial deposits	plain	well	130	3.5	126.5	IV	FERS	GAIA2	TELLUS-5s
CESENA	4	alluvial deposits	plain	well	8.3	3.1	5.2	IV	BRSN	GAIA2	LENNARTZ-1s
FELTRE	2	limestone	relief	spring	/	/	/	/	/	/	/
FONTE	2	sandstone	relief	well	120	7.7	112.3	IV	ASOL	Lunitek ATLAS	TELLUS-5s
GERE	1	fluvio-glacial deposits	valley	well	60	31.3	28.7	ZO	PDN6	Lunitek ATLAS	TELLUS-5s
MASER	2	sandstone	relief	well	157	71.3	85.7	IV	ASOL	Lunitek ATLAS	TELLUS-5s
MEDOLLA	3	alluvial deposits	plain	well	50	3	47	IV	CAVE	GAIA2	TRILLIUM-120s
MILANO	3	alluvial deposits	plain	well	152	18	135	IV	MILN	GAIA2	TRILLIUM-40s
MIRANDOLA	3	alluvial deposits	plain	well	300	5.4	294.6	IV	CAVE	GAIA2	TRILLIUM-120s
MONTELUNGO	1	morainic deposits	hill	well	150	52.8	97.2	ZO	PDN4	Reftek-130	LENNARTZ-5s
NIRANO	4	mudstone	hill	mudhole	11	0	11	ZO	PDN10	GAIA2	LENNARTZ-5s
NIRANO1	4	mudstone	hill	mudhole	11	0	11	ZO	PDN10	GAIA2	LENNARTZ-5s
NORCIA	5	alluvial deposits	valley	well	64	30	34	ZO	PDN11	Reftek-130	LENNARTZ-5s
OPPEANO	3	alluvial deposits	plain	well	60	4.6	55.4	ZO	PDN9	SARA-SL06	SARA-SS08-120s
RECOARO	1	sandstone	relief	spring	/	/	/	ZO	PDN13	Lunitek ATLAS	TELLUS-5s
RECOARO1	1	sandstone	relief	spring	/	/	/	ZO	PDN13	Lunitek ATLAS	TELLUS-5s
RENAZZO	3	alluvial deposits	plain	well	6	1.5	4.5	IV	RAVA	GAIA2	LENNARTZ-5s
SECCHIA	3	alluvial deposits	plain	mudhole	1	0	1	IV	CAVE	GAIA2	TRILLIUM-120s
TOPPO	2	alluvial deposits	valley	well	300	114	186	/	/	/	/
TRIPONZO	5	limestone	crest	well	53	3.1	49.9	ZO	PDN12	Reftek-130	LENNARTZ-5s
VERONELLO	1	fluvio-glacial deposits	hill	well	198	90	108	ZO	PDN1	Lunitek ATLAS	TELLUS-5s
VOBARNO	1	alluvial deposits	valley	well	36	11.2	24.8	IV	VOBA	Lunitek ATLAS	TELLUS-5s
VOLARGNE	1	fluvio-glacial deposits	valley	well	99	50	49	ZO	PDN8	Reftek-130	LENNARTZ-5s